Fermilab Note: **FN-0776-E**

A Large Liquid Argon Time Projection Chamber for Long-baseline, Off-Axis Neutrino Oscillation Physics with the NuMI Beam

Submission to NuSAG

September 21, 2005

D. Finley, D. Jensen, H. Jostlein, A. Marchionni, S. Pordes, P. A. Rapidis*
Fermi National Accelerator Laboratory, Batavia, Illinois

C. Bromberg
Michigan State University, East Lansing, MI

C. Lu, K. T. McDonald
Princeton University, Princeton, NJ

H. Gallagher, A. Mann, J. Schneps
Tufts University, Boston, MA

D. Cline, F. Sergiampietri, H. Wang
University of California at Los Angeles, Los Angelas, CA

A. Curioni, B. T. Fleming*
Yale University, New Haven, CT

S. Menary
York University, Ontario, Canada

* Contact Persons: B. T. Fleming and P. A. Rapidis

Contents

Chapter 1

Executive Summary

Results from neutrino oscillation experiments in the last ten years have revolutionized the field of neutrino physics (see, for example, [1]). While the overall oscillation picture for three neutrinos is now well established and precision measurements of the oscillation parameters are underway, crucial issues remain. In particular, the hierarchy of the neutrino masses, the structure of the neutrino mixing matrix, and, above all, CP violation in the neutrino sector are the primary experimental challenges in upcoming years. A program that utilizes the newly commissioned NuMI neutrino beamline, and its planned upgrades, together with a high-performance, large-mass detector will be in an excellent position to provide decisive answers to these key neutrino physics questions.

A Liquid Argon time projection chamber (LArTPC) [2], which combines fine-grained tracking, total absorption calorimetry, and scalability, is well matched for this physics program. The few-millimeter-scale spatial granularity of a LArTPC combined with $\frac{dE}{dx}$ measurements make it a powerful detector for neutrino oscillation physics. Scans of simulated event samples, both directed and blind, have shown that electron identification in ν_e charged current interactions can be maintained at an efficiency of 80%. Backgrounds for ν_e appearance searches from neutral current events with a π^0 are reduced well below the $\sim$ 0.5-1.0% ν_e contamination of the ν_μ beam [3].

While the ICARUS collaboration has pioneered this technology and shown its feasibility with successful operation of the T600 (600-ton) LArTPC [4], a detector for off-axis, long-baseline neutrino physics must be many times more massive to compensate for the low event rates. We have a baseline concept [5] based on the ICARUS wire plane structure and commercial methods of argon purification and housed in an industrial liquefied-natural-gas tank. Fifteen to fifty kton liquid argon capacity

tanks have been considered. A very preliminary cost estimate for a 50-kton detector is $100M (unloaded) [6].

Continuing R&D will emphasize those issues pertaining to implementation of this very large scale liquid argon detector concept. Key hardware issues are achievement and maintenance of argon purity in the environment of an industrial tank, the assembly of very large electrode planes, and the signal quality obtained from readout electrodes with very long wires. Key data processing issues include an initial focus on rejection of cosmic rays for a surface experiment.

Efforts are underway at Fermilab and a small number of universities in the US and Canada to address these issues with the goal of embarking on the construction of industrial-scale prototypes within one year. One such prototype could be deployed in the MiniBooNE beamline or in the NuMI surface building where neutrino interactions could be observed. These efforts are complementary to efforts around the world that include US participation, such as the construction of a LArTPC for the 2-km detector location at T2K [7].

The 2005 APS neutrino study [1] recommendations recognize that "The development of new technologies will be essential for further advances in neutrino physics". In a recent talk to EPP2010, Fermilab director P. Oddone, discussing the Fermilab program, states on his slides: "We want to start a long term R&D program towards massive totally active liquid Argon detectors for extensions of NOvA." [8]. As such, we are poised to enlarge our R&D efforts to realize the promise of a large liquid argon detector for neutrino physics.

Chapter 2

Introduction

Long-baseline, off-axis neutrino oscillation physics provides the next window into the neutrino sector through measurement of neutrino mixing parameters, mass hierarchy, and CP violation. However, experimental sensitivity for $\nu_\mu \rightarrow \nu_e$ appearance measurements suffer from low statistics. In order to maximize sensitivity to these measurements, a high power, clean, neutrino source must be coupled with a highly efficient detector with good background rejection capabilities.

The newly commissioned NuMI beamline provides the world's most intense neutrino beam at 0.2 MW, upgradable to at least 0.6 MW with changes to the Main Injector Complex, and to 2 MW with the construction of a Proton Driver [8]. Off-axis neutrino beams select lower energy neutrino fluxes with small high energy tails. The combination of these beams with the fine-grained, total absorption calorimetry of LArTPCs bring all the ingredients together to maximize sensitivity to this physics.

This document describes the physics motivation for using these detectors for this physics, as well as a program to realize a massive LArTPC, ideal for these measurements. This program includes a baseline design for a 15 kton[1]detector as a significant first step in long-baseline physics with large liquid argon detectors, and an R&D program to realize this on a timescale to begin taking data in 2012, as suggested by the timeline shown in Figure 2.1.

This case is presented in this document in the following order:

- Chapter 3 provides the physics motivation for off-axis, long-baseline, neutrino oscillation physics using a large LArTPC.

[1]Throughout this document a 'ton' is a metric 'tonne'

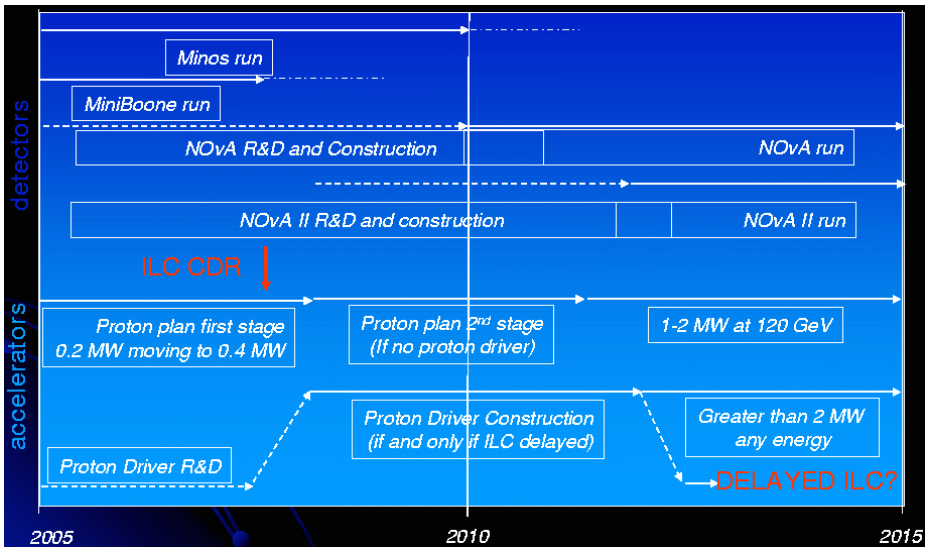

Figure 2.1: Timeline from Fermilab director, Pier Oddone, for neutrino program at Fermilab. Detector technology for 'NOvA II R&D and Construction' referred to as a massive LArTPC. Timeline comes from Pier Oddone's talk to the EPP2010 committee [8]

- Chapter 4 describes events in the detector including efficiencies and event purities.
- Chapter 5 outlines a Baseline Concept for a massive detector.
- Chapter 6 lays out an R&D plan for this program including costs and schedule.
- Chapter 7 outlines initial cost estimates and schedule for the entire project.
- Chapter 8 describes additional physics measurements using large liquid argon detectors.
- Chapter 9 provides a summary and conclusion.

Chapter 3

Physics Motivation

Liquid Argon Time Projection Chambers couple bubble chamber quality imaging with calorimetry and active readout making them ideal detectors for running and future neutrino experiments. The ICARUS collaboration has pioneered efforts to realize this technology as indicated by the successful operation of the T600 detector [4]. This chapter outlines how these detectors work, the ICARUS program's success, and the promise of these detectors for neutrino oscillation physics using the NuMI neutrino beam.

3.1 Liquid Argon TPC Detectors

Liquid Argon Time Projection Chambers image charged particle tracks using their ionization electrons. Passing charged particles ionize in the open volume of liquid Argon. The ionization electrons are drifted over meters to wire chamber planes. Electrons induce signals on initial wire plane(s) rotated with respect to one another to tag the location of the electron in the plane. The final "collection" plane, collects the electrons. Position in the drift direction is determined from drift velocity and drift time. Figure 3.1 shows a schematic of ionization electrons drifting towards readout planes.

With wire chamber pitch of typically 3-5 mm, and readout electronics operating at 2.5 MHz, tracks are imaged with bubble chamber quality precision. In addition, this active readout scheme combines fine-grained tracking with total absorption calorimetry.

These detectors are ideal for low rate neutrino physics. In particular, interactions from low energy neutrino beams, below deep inelastic scattering threshold, are clean

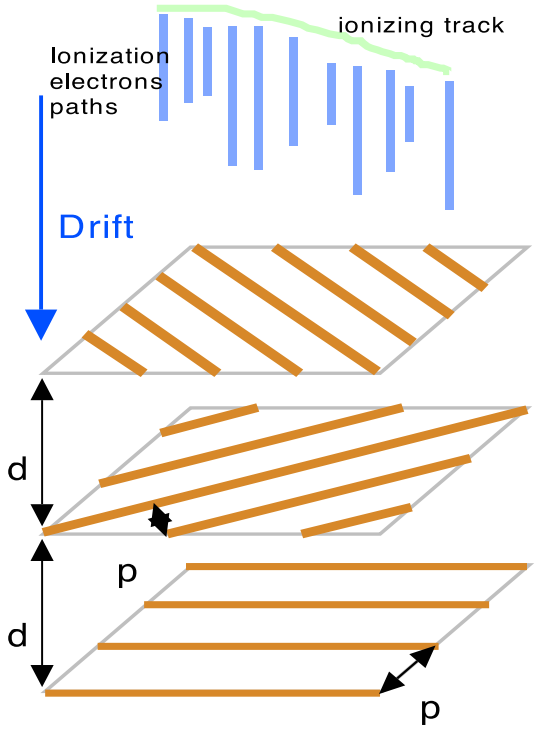

Figure 3.1: Ionization electrons induce signals on the first two readout planes and are collected on the third "collection" plane. Distances d and p are ∼3-5 mm.

events that are relatively easy to unfold and reconstruct.

3.2 Status of ICARUS

In the 1980s, the ICARUS collaboration began an intense R&D effort to realize this detector concept. A series of small prototypes was constructed [9, 10, 11] to understand, among other things, charge and light production, argon purity, charge collection, etc, in these kinds of detectors. This R&D program led to the successful construction of the T600 which operated for 3 months on the surface in Pavia in 2001 [4]. This detector, recently re-located to the Gran Sasso laboratory, is expected to again be operational starting the summer of 2006. Recently the INFN president indicated that instead of completing the ICARUS plan to upgrade this detector to 1800 tons, the group should abandon the modular ($\sim$300 tons/module) technology and develop an approach which can be scaled to massive detectors. While the T600 begins operation in the Cern to Gran Sasso beam as a proof of principle, proposals for larger detectors will be considered.

With the success of the T600 detector, the ICARUS collaboration has brought this technology to maturity. Open questions remain in scaling these detectors up to what is appropriate for long-baseline physics goals, but the motivation for using these massive detectors for this physics is clear, as is laid out in the next section.

3.3 Long-Baseline Off-Axis Neutrino Physics Sensitivity

The remarkable results from the last decade of neutrino physics have revealed an unexpected picture of neutrino oscillations and neutrino mass. These results have brought many more questions, such as: How does neutrino mass arise? What is the pattern of masses and mixings in the neutrino sector and what does this tell us? Is there CP violation in the neutrino sector that can help to explain the matter anti-matter asymmetry in the universe? These questions and more are the focus of intense study in the neutrino community. In particular, long baseline neutrino oscillation physics can probe not only the pattern of masses and mixings, but also search for CP violation in the neutrino sector. The 2005 APS Neutrino Study recognizes the importance of this physics program, recommending it as one of the three highest priorities in the field [1]:

> "We recommend, as a high priority, a comprehensive U.S. program to complete our understanding of neutrino mixing, to determine the character of the neutrino mass spectrum, and to search for CP violation among neutrinos. This program should have the following components:
>
> - An expeditiously deployed multi-detector reactor experiment with sensitivity to $\overline{\nu_e}$ disappearance down to $\sin^2 2\theta_{13} = 0.01$, an order of magnitude below present limits.
> - A timely accelerator experiment with comparable $\sin^2 2\theta_{13}$ sensitivity and sensitivity to the mass-hierarchy through matter effects.
> - A proton driver in the megawatt class or above and neutrino superbeam with an appropriate very large detector capable of observing CP violation and measuring the neutrino mass-squared differences and mixing parameters with high precision."

The sensitivity of these long-baseline, off-axis $\nu_\mu \rightarrow \nu_e$ appearance experiments depends on the number of ν_e's observed above background. Statistical sensitivity, S, depends upon detector mass, detector efficiency, number of protons on target per year, and number of years run. Backgrounds for the ν_e appearance search include intrinsic ν_e's in the beam and mis-identified neutral current π^0 interactions. Massive LArTPCs are ideal for this physics in that they have both very high ν_e efficiency (∼80-90%) and effectively complete background rejection of neutral current π^0 interactions, as described in Chapter 4. By comparison, scintillator and Čerenkov based experiments have ∼25% ν_e efficiency with a neutral current π^0 background about the same size as the intrinsic ν_e background. The relative sensitivities for the two types of detectors is illustrated in recent work by Mena and Parke [12]. They consider three classes of experiments referred to as "small", "medium", and "large". Each type is defined for NOνA and for a massive LArTPC for sensitivity calculations. Table 3.1 describes these definitions.

Using these definitions, sensitivities are calculated for reach in $\sin^2 2\theta_{13}$ vs. $\sin\delta$ for neutrino running, anti-neutrino running, and the combination of the two. Three year runs in each mode with 7.5×10^{20} protons on target per year is assumed. For each sensitivity, different combinations of the mass hierarchy and sign of $\cos\delta$ are considered. These sensitivities are shown in Figures 3.2 and 3.3 for neutrino and anti-neutrino mode respectively with the combination of both runs shown in Figure 3.4.

Sensitivity to determination of the mass hierarchy is shown in Figure 3.5.

	Small	Medium	Large
NOνA	30kton	30kton + Proton Driver or (5 times mass or exposure)	30kton + Proton Driver + (5 times mass or exposure)
LArTPC (with 90% ν_e efficiency)	8kton	40kton	40kton + (Proton Driver or 5 times mass or exposure)

Table 3.1: Definitions of "small", "medium", and "large" for sensitivity studies from recent Mena and Parke paper [12]

There is clearly a great advantage to using massive LArTPCs for this physics due to, most importantly, excellent ν_e efficiency, and excellent background rejection. With a baseline concept for a massive LArTPC laid out in Chapter 5, and an R&D plan to achieve this described in Chapter 6, a massive LArTPC can be realized for long-baseline, off-axis physics using the NuMI beam.

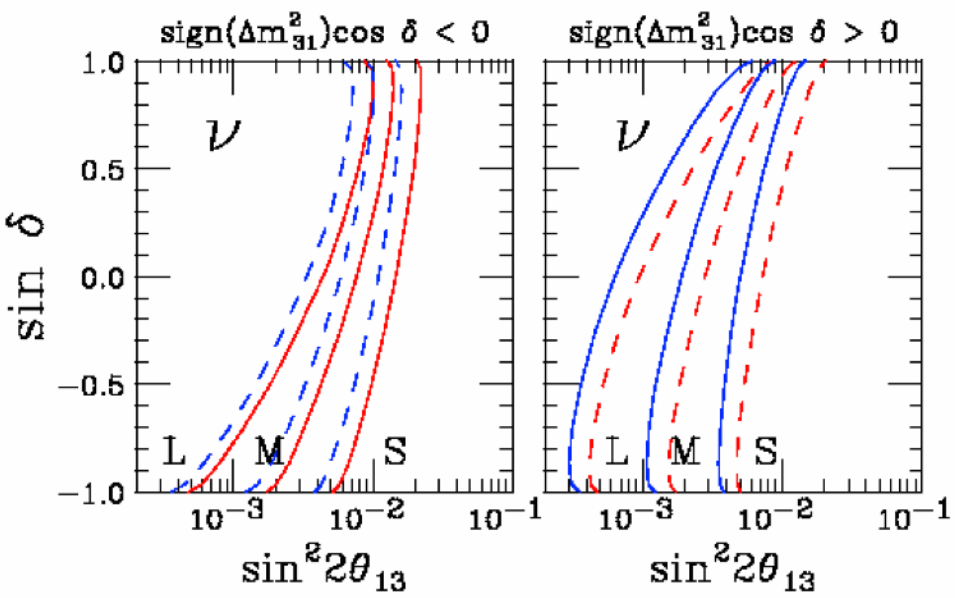

Figure 3.2: Sensitivity to $\sin^2 2\theta_{13}$ vs. $\sin\,\delta$ for "small", "medium", and "large" detectors for three years running in neutrino mode, assuming 7.5 $\times 10^{20}$ protons on target per year. The plot on the left assumes the most restrictive case with, in blue, the assumption that $\cos\,\delta < 0$ and the normal hierarchy, and in red, the assumption that $\cos\,\delta > 0$ and the inverted hierarchy [12].

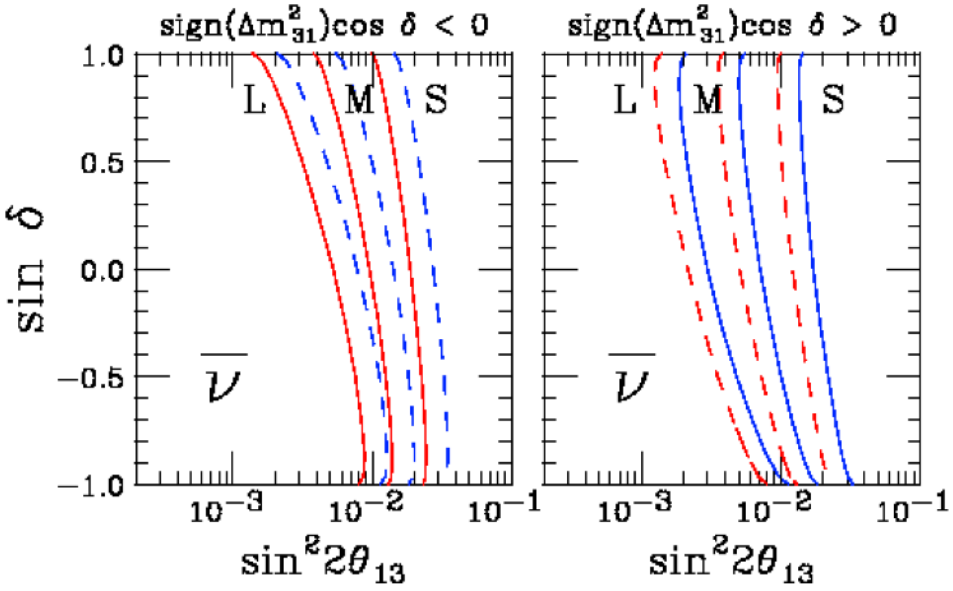

Figure 3.3: Sensitivity to $\sin^2 2\theta_{13}$ vs. $\sin\,\delta$ for "small", "medium", and "large" detectors for three years running in anti-neutrino mode, assuming 7.5 $\times 10^{20}$ protons on target per year. The plot on the left assumes the most restrictive case with, in blue, the assumption that $\cos\,\delta < 0$ and the normal hierarchy, and in red, the assumption that $\cos\,\delta > 0$ and the inverted hierarchy [12].

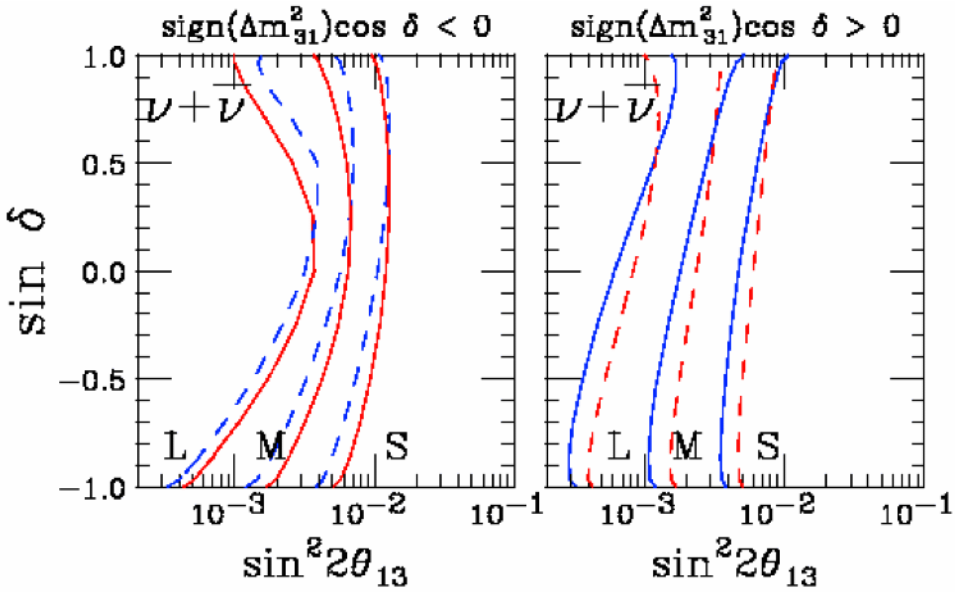

Figure 3.4: Sensitivity to $\sin^2 2\theta_{13}$ vs. $\sin\,\delta$ for "small", "medium", and "large" detectors for three years running in neutrino mode combined with three years running in anti-neutrino mode, assuming 7.5 $\times 10^{20}$ protons on target per year. The plot on the left assumes the most restrictive case with, in blue, the assumption that $\cos\,\delta < 0$ and the normal hierarchy, and in red, the assumption that $\cos\,\delta > 0$ and the inverted hierarchy [12].

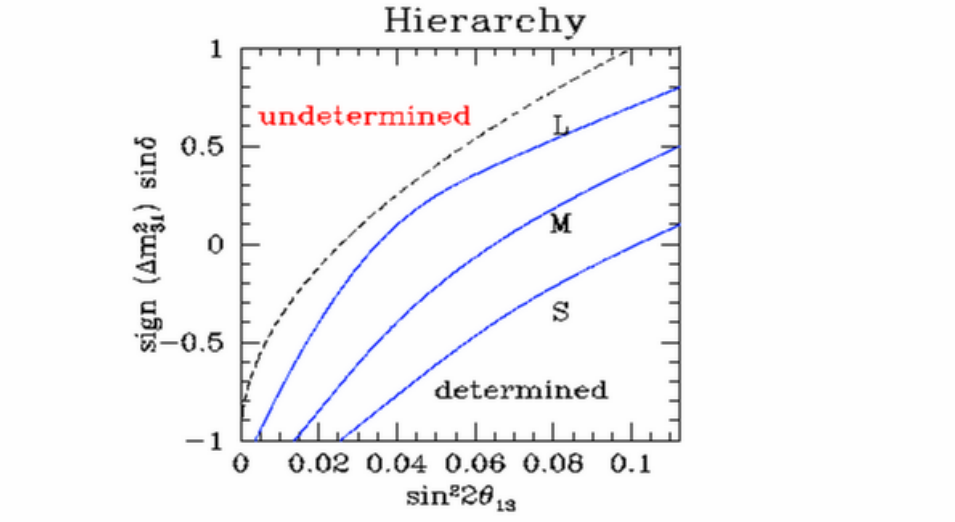

Figure 3.5: Sensitivity for determination of the neutrino mass-hierarchy for "small", "medium", and "large" detectors [12].

Chapter 4

Event Simulation and Detector Capabilities

In this chapter we present the results of Monte Carlo studies to determine the signal efficiency and background rejection capabilities of a liquid argon TPC detector located in the NuMI off-axis beam.

4.1 Software and Simulations

A series of Monte Carlo studies has been carried out using the Liquid Argon Interactive Reconstruction (LAIR) program written by Adam Para and Robert Hatcher [13]. The program is based on GMINOS, the GEANT 3 Monte Carlo program originally developed for the MINOS experiment and which has also been used by the NOνA experiment. Event samples were prepared by Adam Para and involved a full GEANT 3 simulation of the events. The event generator NEUGEN3 was used [14]. This program simulates all single pion production backgrounds and has been used by the Soudan 2, MINOS, MiniBooNE, MINERνA, and NOνA experiments. In the energy range of interest for off-axis oscillation studies the predictions for single pion production from the program have been compared to previous bubble chamber results as well as to more recent data from the Soudan 2 and MiniBooNE collaborations. The fluxes are those for 11 km off-axis location 820 km away. Oscillated event samples were generated with $\Delta m^2 = 2.5 \times 10^{-3} eV^2$. For most studies an energy pre-selection was applied such that events with a visible energy outside of the energy window from 1.5 to 4.5 GeV were rejected. An energy cut of this type would certainly be applied to any real analysis as it focuses on the expected signal region, reducing the background

from beam ν_e by a large factor and reducing the neutral current (NC) event rate by a factor of six [15].

4.2 Simulated Events

Figures 4.1 and 4.2 show two images of the same event. The first is the event in a LArTPC detector, as simulated by the LAIR GEANT 3-based Monte Carlo. In the second, hits have been averaged over multiple liquid argon samples to approximate the imaging of the NOνA detector. The lower photon shower, clearly identifiable in liquid argon based on the displacement from the vertex and the high pulse height at the shower start, is much more difficult to identify correctly with degraded imaging.

Figure 4.3 shows a typical high energy NC event. This event is from a high energy neutrino producing a shower with 9 GeV of energy, most of which goes to two charged pions which are clearly visible. A 1.1 GeV π^0 is also produced; the two photon showers are clearly visible, as is their pointing to the event vertex. Notice the difference in pulse height between the MIP tracks and the start of either shower. The red hits indicate energy deposition roughly twice that of a MIP particle. The ability to distinguish photon-induced from electron showers on the basis of average ionization on the initial, track-like segment of the shower, is a crucial strength of the technology.

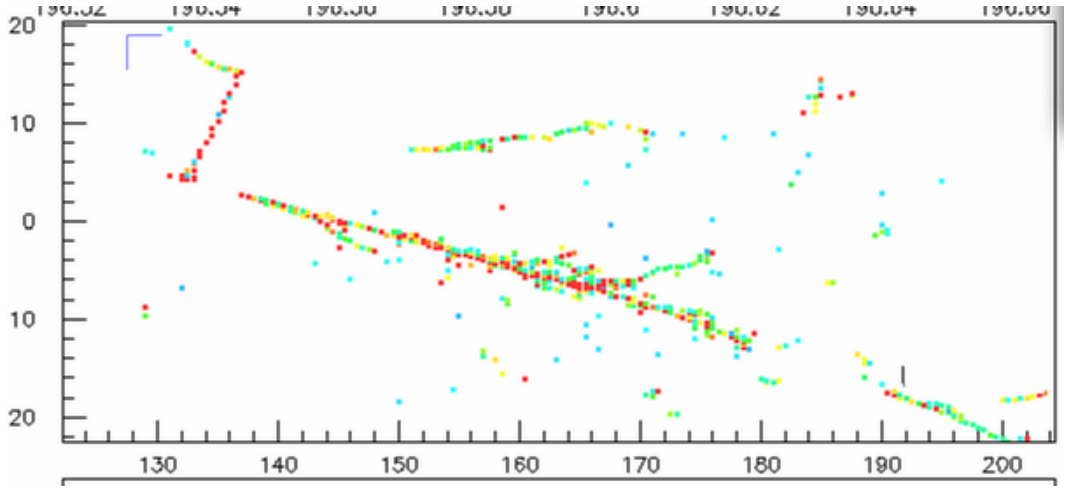

Figure 4.1: A simulated neutral current event with a 1 GeV π^0 ($\nu_\mu + n \rightarrow \nu_\mu + \pi^+ + \pi^- + \pi^0 + n$). Sampling rate is every 3.5% of a radiation length in all three views.

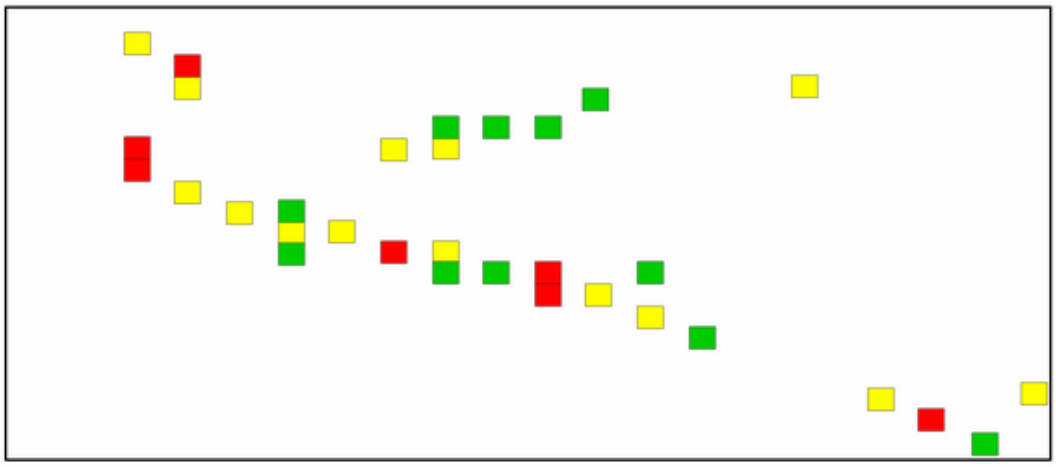

Figure 4.2: The same event as in Figure 4.1 where the hits have been averaged to approximate the imaging capabilities of the NOνA detector. Sampling rate is every 12% of a radiation length in alternating x-y planes.

4.3 Studies of Signal Efficiency and Background Rejection

In order to quantify the signal efficiency and background rejection of a large LArTPC detector, the Fermilab, Michigan State, and Tufts groups have undertaken a set of studies based on hand scanning of events. Scanning studies at this point serve several functions:

1. Once a scanner is trained, and can identify the characteristic topologies and event features produced by specific kinds of interactions, it is easy to make a quick estimate of the signal efficiency and background rejection factors.

2. A successful scan effort allows one to define a set of "scan rules" which can then serve as the basis for software. In addition, the most challenging aspects of pattern recognition can be identified and studied separately.

3. Scan analysis provides qualitative feedback for the detector optimization studies, in particular which aspects of the detector performance (noise, hit inefficiency, drift or dE/dx uniformity) are most important for pattern recognition.

The groups participating in the study have relatively recent experience with hand scanning from the Soudan 2 and DONUT experiments, both of which used it at an intermediate step in the analysis.

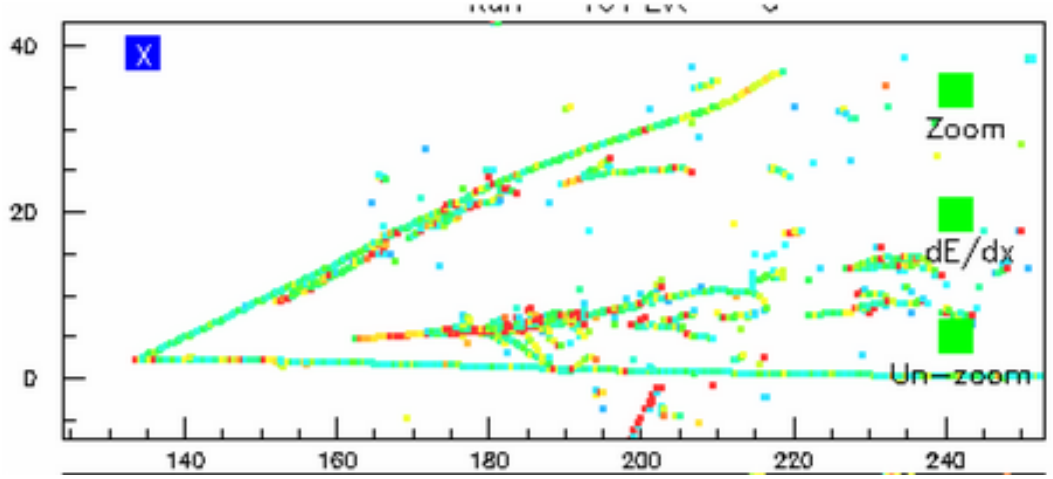

Figure 4.3: A neutral current event with over 8 GeV of visible energy. Visible are two charged pion tracks and two showers from a π^0.

Methodology

For the Tufts study four undergraduate students from J. Schneps undergraduate E&M class volunteered to participate in the project. Over the 2005 spring semester they worked 5-10 hours per week scanning and reconstructing events. These students, two sophomores and two juniors, had no previous exposure to particle physics. In preparation for the blind scan the students underwent a training program consisting of the following:

1. General introduction to particle detectors, neutrinos, and characteristic topologies produced in LAr by various particles.

2. Introduction to LAr detectors, stereo geometry and software. Students scanned single particle events with single electrons, muons, and photons of known energy and angle in the detector. This process helped motivate the difference between e and γ-induced showers. The single muon files were invaluable in understanding the geometry of the stereo views.

3. Scanning samples of around 50 events from each of ν_e and ν_μ CC and NC samples.

4. Scanning samples of around 50 ν_e events, both NC and CC, checking results against truth. Repeat a few times with varying amounts of input from "experts".

Event Type		N	pass	ϵ	η
NC		290	4	-	0.99±0.01
signal ν_e	CC	32	26	0.81±0.07	-
Beam ν_e	CC	24	14	0.58±0.10	-
Beam ν_e	NC	8	0	-	/
Beam $\overline{\nu}_e$	CC	13	10	0.77 ± 0.09	-
Beam $\overline{\nu}_e$	NC	19	0	-	/
ν_μ	CC	32	0	-	/
$\overline{\nu}_\mu$	CC	32	1	-	/

Table 4.1: Scan results for various event categories. ϵ is signal efficiency and η is the background rejection efficiency. "/" indicate samples where the event size is too small to draw meaningful conclusions.

5. Scanning several dozen events from specially selected "hard" samples: $y > 0.8$ ν_e CC events, NC events with 3 or more π^os.

Once the training process was completed, students scanned a sample of 450 events. Each event was scanned independently by 2 students and was assigned a score from 1 (sure background) to 5 (sure signal). The students then compared their results, and scanned as a group any events where their individual scores differed by more than one unit, or other events flagged as meriting further scrutiny. Events receiving a score of 3 or higher by at least one student were considered to pass the student scan and were then scanned by the experts for final classification. The expert scan was carried out by at least two of Gallagher, Mann, Schneps, and assigned a binary signal/background decision to each event.

Results

Figure 4.4 shows the scan scores for events from the true NC, ν_μ CC and ν_e CC samples. The scores independently assigned to each event by the two scanners were very similar. In all, 282 of 290 NC events and 27 of the 32 CC events had scan scores differing by no more than one unit. This suggests that the scanners were applying the same set of criteria in making their event classifications and agreeing on the topological features that served as the basis for their event classification decisions. The latter bodes well for the prospects of converting the decision making procedures employed by the students to software algorithms.

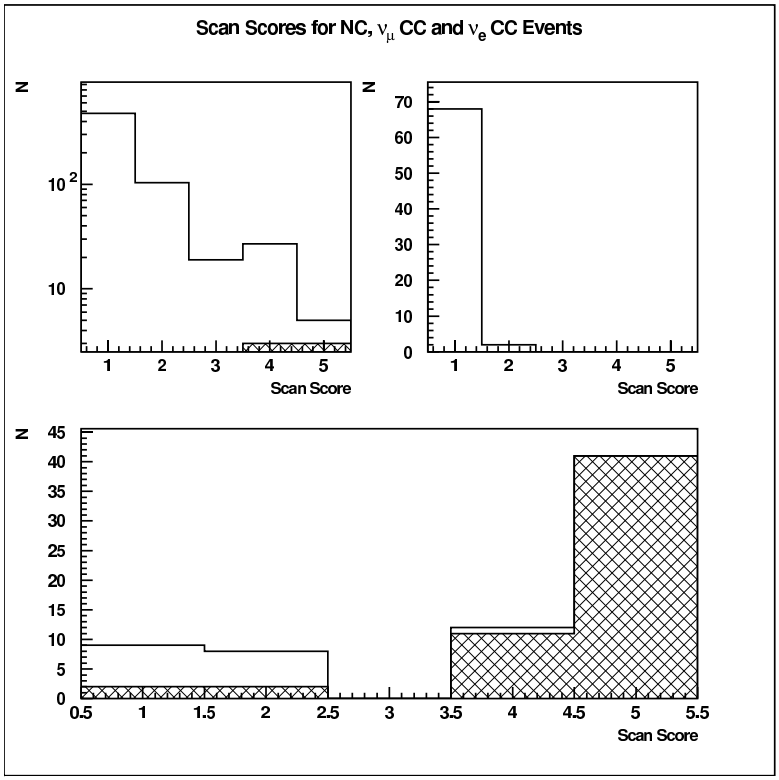

Figure 4.4: Student scan scores for events in the NC (top left), ν_μ CC (top right), and ν_e CC samples. Hatched histogram indicates the events flagged as "signal" in the expert scan. Since each event is scanned independently by two students, each event contributes two entries to each histogram. Note the log scale on the NC distribution.

Table 4.1 shows the numbers of events from each sample to be classified as signal through the two scans. 26/32 signal events and 4/290 NC events passed the scan analysis for a signal efficiency of 81±7% and a background rejection efficiency of 99±1 %. Combined with the factor of 6 rejection on NC background coming from the energy pre-selection, the total NC rejection efficiency is 99.8%. Figures 4.5 and 4.6 show the event characteristics for the CC ν_e signal and CC ν_e beam background. In each plot the top histogram is the full sample and the hatched histogram are events that pass the scan. The signal efficiency as a function of y can be roughly characterized as 100% below y of 0.5, and still nearly 50% for $y > 0.8$. The fact that high-y showers tend to be at large angles, and therefore spatially separated from other activity in the event, provides a compensating advantage for these events.

A difference is seen in the signal efficiencies between the signal ν_e CC events and those from the ν_e beam background, 81±7% vs. 58±10%. An examination of the energy distributions in Figures 4.5 and 4.6 may provide a partial explanation. The

background distribution shows (with low statistics) a possible energy dependence to the signal efficiency, as 0/4 events with energy greater than 3.5 GeV made it through the scan. This energy dependence may be partly the result of bias in the training based on the samples used.

These results are consistent with a second scan study that was carried out independently at Michigan State. In this study a set of classification criteria were defined based on inputs like the number of showers in the event, distance from the vertex to the start of the shower for electron candidates, and average pulse height on the electron candidate track. These criteria were then applied to a sample of 50 signal and 35 background events, of which 41 CC events and zero background events passed. The signal efficiency of 82±6% is consistent with the previous result.

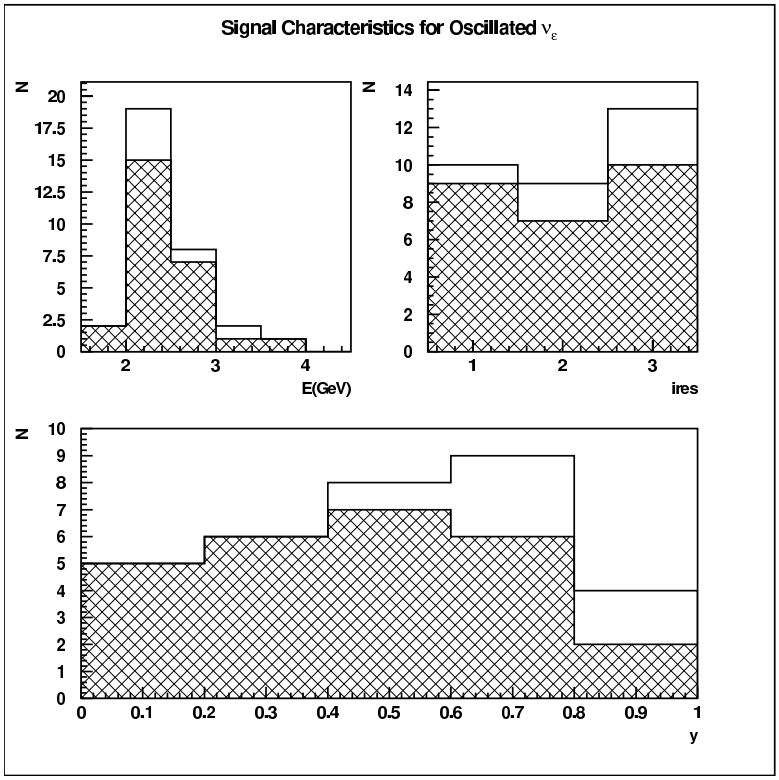

Figure 4.5: Event characteristics for ν_e CC events selected from the oscillated parent distribution. Solid histograms are all events, hatched are those which were passed as signal through the 2 scans. **Top Left: Neutrino Energy. Top Right: Interaction type (quasi-elastic, resonance production, DIS). Bottom: y.**

Figure 4.7 shows an event display of a high-y event that passed as signal in the analysis. The event received a "4" score from both scanners. Though the shower is relatively low energy, the fact that it is spatially separated from the rest of the event

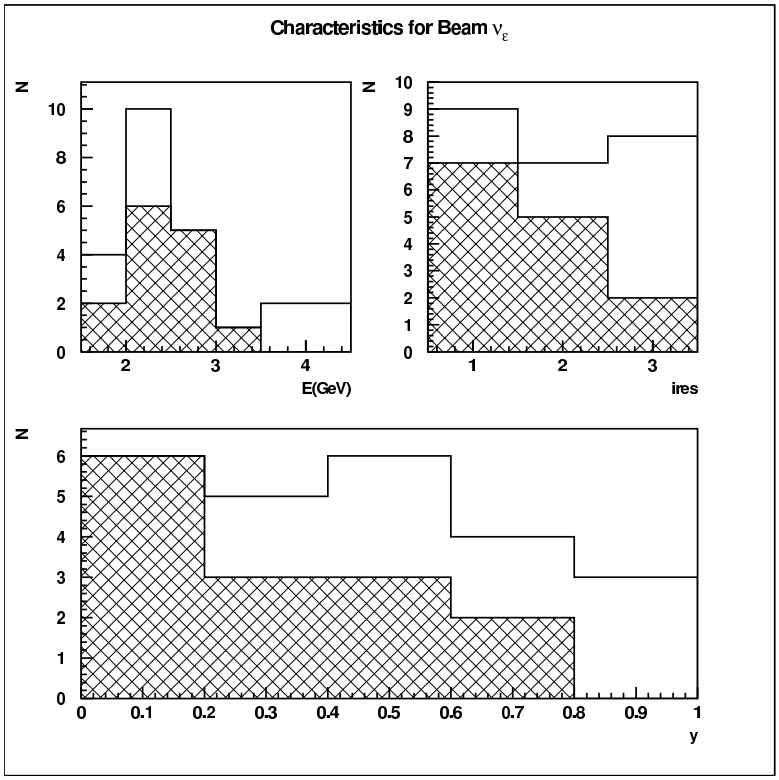

Figure 4.6: Event characteristics for ν_e CC events selected from the ν_e beam background distribution. Solid histograms are all events, hatched are those which were passed as signal through the 2 scans. **Top Left: Neutrino Energy. Top Right: Interaction type (quasi-elastic, resonance production, DIS). Bottom: y.**

makes positive identification possible.

4.4 Conclusions and Future Work

Two independent scan-based analyses have been carried out to quantify the signal efficiency and background rejection of a LArTPC detector in the NuMI offaxis beam. The results of the two analyses are completely consistent. In a blind scan of 450 events the signal efficiency and background rejection for NuMI off-axis events in a LArTPC detector with a pre-selection on visible energy are found to be 81%±7% and a background rejection of 99±1 %. These results were obtained in a blind scan carried out in two stages, the first by a group of undergraduates and a second by physicists who reviewed all events passed in the first stage. The accepted events therefore comprise the AND of the two scans.

The next step for simulations studies will be to develop software based on the

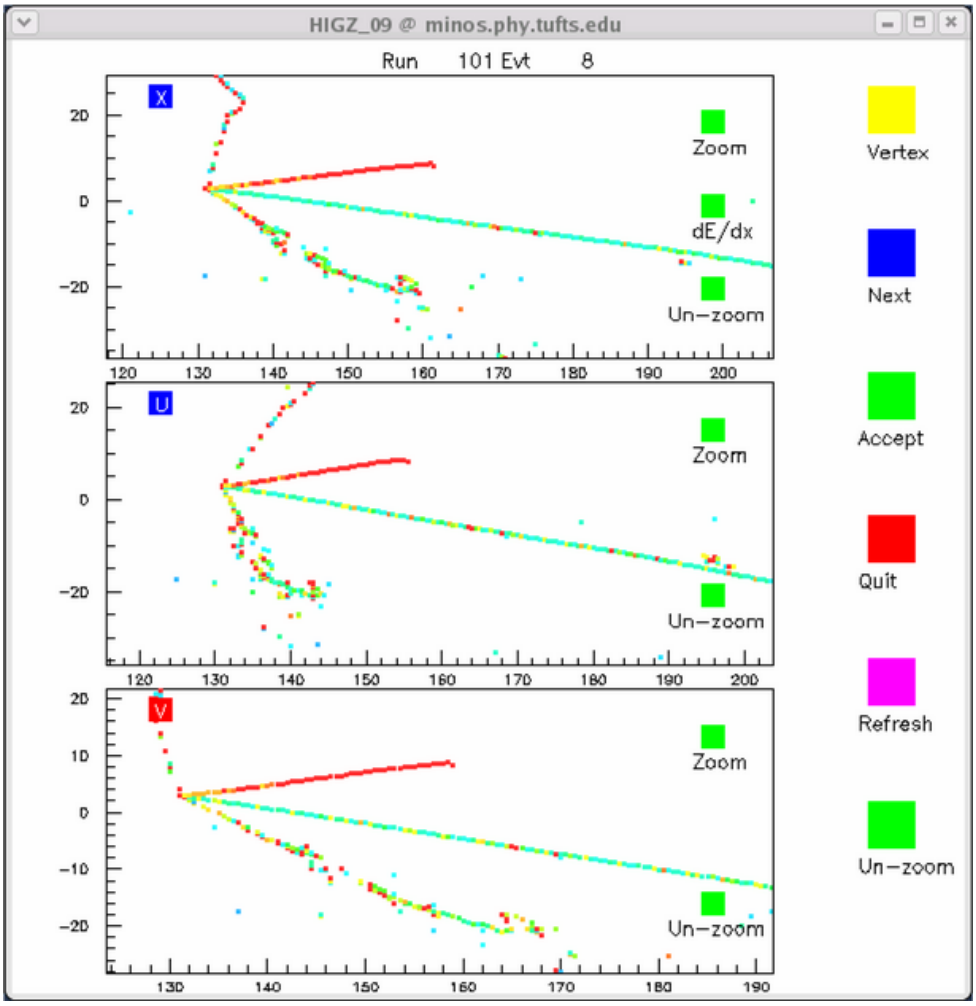

Figure 4.7: Signal event selected, 2.2 GeV DIS ν_e CC with y=0.89. The electron shower is clearly visible.

criteria identified in the scan studies. Because of the abundance of information present in these events developing the sophisticated pattern recognition and machine learning approaches required to extract the maximum sensitivity from this technology will be a challenge. The initial guidance provided by these early scanning-based studies will be important in developing the reconstruction software that will be required for the next round of Monte Carlo studies, which will be needed for optimizing detector design.

Chapter 5

Baseline Concept

The baseline concept for a 15 kton LArTPC to address the physics goals laid out in Chapter 3 is described here. A large Liquified Natural Gas (LNG) storage tank system serves to house the detector. The outer tank cylinder is 29.1 m in diameter and 25.6 m high; the insulated inner tank which contains the 15 ktons of LAr is 26 m in diameter and 21.2 m high.

The design employs a total of 8 distinct drift regions formed by 4 sections of signal wires interspersed between 5 cathode planes. Each drift region is 3 meters from cathode to signal wires and is surrounded by a field cage to create a uniform field for the drifting electrons. The drift field is 500 V/cm giving a drift velocity of 1.5 m/ms and a maximum drift time of 2 ms.

Each section of wires contains 2 sets of three wire planes (one set for the drift region on each side). Within each set, the outermost two planes are induction planes strung at $\pm$ 30 degrees from the vertical, and the innermost plane is a vertical collection plane. (A description of induction and collection planes is given in [4].) The wires are 150 μm stainless steel. The wire pitch is 5 mm and the spacing between planes is 5 mm. Only wires that reach the top of the detector are read out, giving a total of 110,000 channels. This gives three plane (overconstrained) coverage on part of the detector volume and two plane coverage (vertical plus one angle) everywhere else.

The wire and cathode planes hang from trusses which are just below the roof of the inner tank and are supported by the wall of the inner tank. The signals are piped out via $\sim$ 50 chimneys emerging through the roof of the inner vessel. The electronics and Data Acquisition System (DAQ) are in an accessible region on a floor above the inner vessel. Figure 5.1 shows the outer tank, the inner tank and the arrangement of

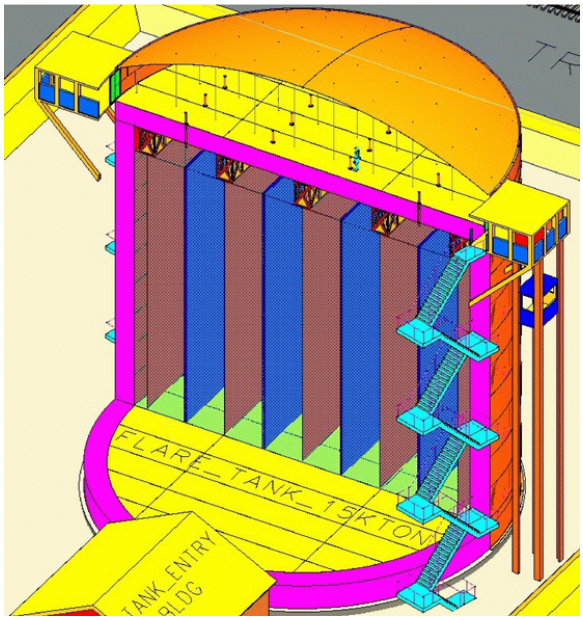

Figure 5.1: Rendering of interior of 15 kton vessel showing outer tank, inner tank, wire and cathode planes, and signal chimneys.

the electrodes. Figure 5.2 shows the arrangement of the field cages and the chimneys which carry the signals to the electronics.

The argon is maintained in thermal equilibrium by a system of liquid nitrogen condensers in the vapor region at the top of the inner tank. The argon purity is maintained and improved by a recirculating purification system operating on the liquid in the tank.

In the sections below, details on the tank and inner structure are described as well as issues related to argon purity, electronics readout and data acquisition.

5.1 Tank and Inner Structure

Liquid argon will be contained in a double wall, flat bottom, insulated, cryogenic storage tank similar to tanks commercially built for the liquid natural gas (LNG) industry. While the tank for the LAr application will share most of the basic design with the commercially produced tanks, key modifications will be made to the upper portions of the tank to allow the tank to provide the structural support for the detector wires.

The American Petroleum Institute (API) has developed a standard applicable to double wall, flat bottom insulated cryogenic storage tanks titled API 620Q. The Tank

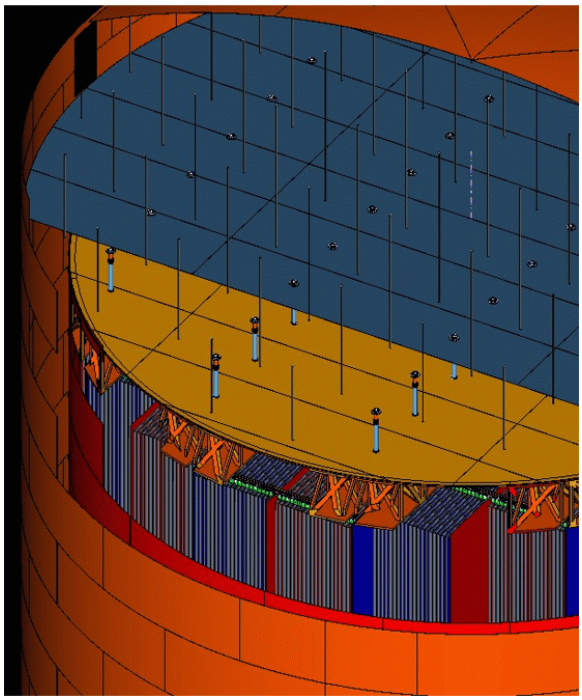

Figure 5.2: Rendering of the interior of the 15 kton vessel showing field cage structure.

used for this project will meet the requirements of this standard. Key similarities and differences between the tanks used in industry and the tank proposed for LAr are:

Similarities:

- Industrial tanks are built both much larger and slightly smaller than the LAr tank proposed here.
- Operating pressures for both industrial tanks and this LAr tank are approximately 3 psig. These are not considered to be within the scope of the ASME boiler and pressure vessel code since the operating pressure is less than 15 psig. Relief valves for both pressure and vacuum are required.
- Several relief valve manufacturers provide vacuum and positive pressure relief valves used on API 620Q tanks. These same valves will be installed on this tank.
- Industrial tanks use the same material of construction (9% Nickel steel) for the inner shell as that proposed here. The outer shell (warm sections) of these tanks is routinely constructed of ordinary carbon steel plates.
- Industrial tanks routinely operate at temperatures both above (LNG @ 110K) and below (LN2 @ 80K) the temperature of liquid argon (@87 K).

- Expanded perlite insulation is used to insulate the sides and top while polyurethane foam blocks are used for insulating the bottom of industrial tanks. These same insulation materials will be used for the LAr tank.
- Heat gain into double wall flat bottom storage tanks typically results in boil off rates of less than 0.05% per day. This boil off rate would be applicable to the LAr tank also.
- Multiple national and international construction firms routinely contract for the fabrication and erection of the API 620Q tanks and would be capable of providing the LAr tank.
- Construction means and methods are identical.
- All double wall flat bottom tanks are custom designed for the customers specific application. Foundations are individually designed for the specific soil conditions and tank product and liquid height. Foundation heating is usually incorporated in the foundation design to prevent frost heave of the foundation.
- Tank erectors routinely leave door sheets (large 20 foot wide by 10 to 20 foot tall) open in the shell of both the inner and outer tank during construction to allow adequate access.
- External and internal stairways are frequently included in industrial API 620Q tanks and would be specified for the LAr tank.

Differences:

- Industrial tanks usually contain liquids with a specific gravity of approximately 0.6 where the specific gravity of liquid argon is 1.4. Therefore, the thickness of the inner tank shell plates will be increased to accommodate the higher loads. The shell plate thickness sizing criteria have been very well understood for approximately one hundred years.
- Non-destructive examination (NDE) techniques for testing standard API 620Q tanks are applicable to the LAr tank. Because the standard hydrostatic tests result in less structural loading than results for loading of argon, additional NDE (radiography, ultra-sonic examination) will be specified for the LAr tank.
- The structural modifications (trusses, stiffeners) to the top of the inner tank which allow the tank shell to take the structural loads for the detector wires

in the LAr application are atypical of the standard industrial tank. However, the materials and construction techniques are well understood in the structural steel industry.

- The LAr detector tank will include a habitable area above the insulation space above the liquid argon. Industrial API 620Q tanks do not include normally occupied areas, but do routinely include accessible areas atop the outer tank roof. In industrial tanks, equipment such as pumps, valves, and instrumentation are accessed from the roof of the outer tank. One national steel plate structure fabrication firm (PDM) routinely placed habitable space in the column area of fluted column elevated water towers. Examples are located in Downers Grove and Alsip, Illinois.

- A properly rated elevator will be specified to allow easy personnel access to and egress from the attic portion of the LAr tank. Elevators are not usually installed in industrial API 620Q tanks, but are frequently included in the annular space between smokestack lines and an outer smoke stack (which are frequently erected by the same contractors that erect double wall flat bottom tanks). Such elevators are typically rack and pinion drive units similar to the units installed at MINOS and NuMI service buildings.

	Nominal Capacity, ktons (metric):	10	15	20	25	50
	Inner Tank Diameter, meters	26	26	26	26	40.75
	Inner Tank Diameter, feet	85.31	85.31	85.31	85.31	85.31
	Inner Tank Height, meters	14.88	21.20	28.39	35.15	28.27
	Inner Tank Height, feet	48.82	70.99	93.15	115.32	92.74
	Outer Tank Diameter, meters	29.10	29.10	29.10	29.10	43.66
	Outer Tank Diameter, feet	95.49	95.49	95.49	95.49	143.2
	Outer Tank Height, meters	18.9	25.6	32.61	39.92	32.92
	Outer Tank Height, feet	62.0	84.0	107.0	129.0	108.0

Table 5.1: Tank specific overall dimensions for a range of tank sizes from 10-50 ktons:

5.2 Argon Cooling, Supply, and Purification

A detailed description of the cooling system for the liquid argon in the tank is given in reference [16]. In summary, the heat conducted through the tank-walls, feedthroughs

and other sources is removed by liquid-nitrogen filled re-condensers in the ullage (gas volume) above the liquid in the detector tank. The heat-load has been estimated at 34 kW and is removed by 5 re-condensers each with $2m^2$ of surface and a volume of $0.3m^3$. Commercial refrigerators are available to handle this load and the system is expected to use some 15 tons of Nitrogen/day - 6 trucks or 2 rail cars per week.

Safeguards will be implemented to deal with a malfunction of the cooling system or a long interruption in Nitrogen delivery. (A local generator system will take over in case of a power outage). As per [16], in case of a failure, the boil-off rate will be 0.5 tons/hour and provision will be made to vent the excess gas in such a way as to prevent air entering the tank either as backflow or during recovery.

There are 5 major suppliers of argon in the U.S and our 15 ktons represents about 1.5% of annual production in the U.S. We have contacted two vendors both of which stated that they could supply such an amount over a period of 4 months. Based on the prices and availability we have been quoted, we have not pursued the notion of having our own production plant. This decision could be revisited if necessary. The argon can be brought either by road or by rail; there is a small cost advantage in rail. The argon will be tested on arrival. Unsatisfactory lots will be returned; satisfactory material will pass through a purifier and be stored in a buffer tank before transfer to the detector tank.

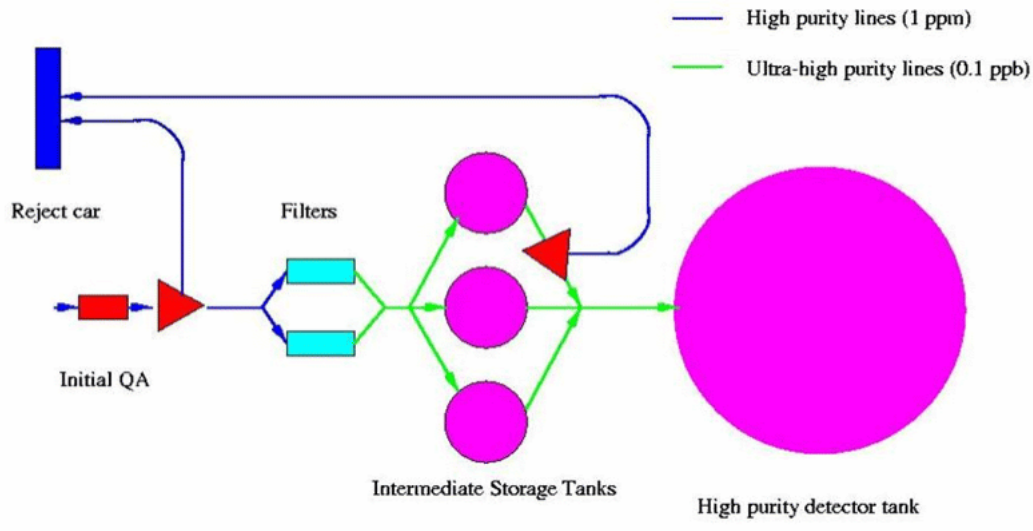

Figure 5.3: Schematic of argon receiving

A key advantage of a LArTPC detector stems from the fact that it is possible to drift ionization electrons over a distance of meters and thus to instrument a relatively large mass of detector per readout channel. To avoid too much loss of signal between

the point of ionization and the readout electrode, however, the argon must not contain O_2 and similar electro-negative impurities above a certain level. The drift lifetime for our range of drift fields can be parametrized as $\tau_{\rm drift}({\rm ms}) = \frac{0.3\times10^{-9}}{({\rm Oxygen\ \ concentration})}$. The largest drift time is 2 ms and taking a 20% signal loss as acceptable implies a lifetime of 10 ms or an impurity concentration of 30 parts per trillion (or 30×10^{-12}). Fortunately, these levels are quite achievable. Using custom-built systems, the ICARUS collaboration has demonstrated lifetimes greater than 10 ms [17] and over the past few years, commercial units have been developed for the electronics industry [18] which can deliver these purities starting from commercially available argon.

While we will use commercial Oxygen monitors as a preliminary test, our primary gauge of argon quality will be a number of 'purity' monitors as developed for ICARUS [4, 19]. This device measures the lifetime of drifting electrons, the quantity of interest, and avoids the problems which can arise if we use monitors that test only for a fixed set of contaminants. Figure 5.4 shows a lifetime monitor and a plot from ICARUS showing a comparison of drift lifetime as obtained from a purity monitor and as obtained from signals tracks with known drift distances. The agreement is excellent.

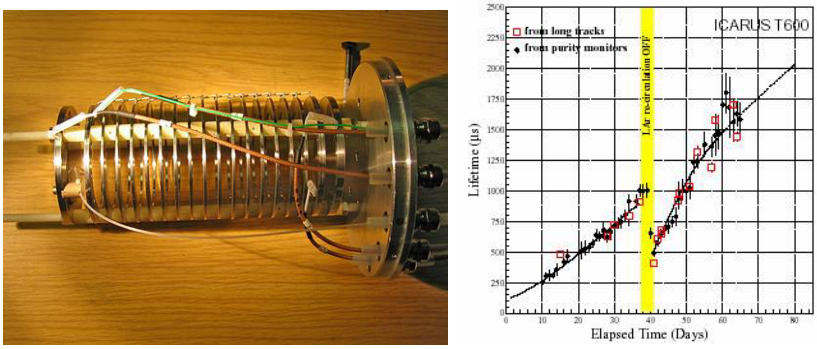

Figure 5.4: A purity monitor and a comparison of drift lifetime as given by a purity monitor and as derived from signals from long tracks [20].

Our detector design does present a set of challenges to achieving the required argon purity. The initial challenge is to remove the ∼2.5 tons of Oxygen in the tank atmosphere; previous detectors have evacuated their cryostats but this is not feasible in this case. The walls of the tank, the cables and detector components will be made of non-contaminating materials but their outgassing will be a source of H_20 and O_2. It will also be critical to minimize any leakage of air into the tank and to avoid any contamination from components in the detector and the argon transfer lines.

Taking the last two issues first, the tank will be subject to the tests described in the tank section. All feed-throughs will also be tested and the perlite insulation surrounding the tank will be purged with dry argon. The components for the argon transfer lines (pumps, valves, piping etc.) will also be certified. The preparation of the tank walls, beyond a thorough washing, will depend on the results of the material tests described in the R & D section.

A scheme for removing the oxygen in the tank atmosphere to the part per million level has been developed by R. Schmitt, a senior cryogenic engineer at Fermilab. It is based on a catalytic process which cycles the tank atmosphere over a Palladium catalyst with a $\sim$3% stream of hydrogen to form water. A tank volume can be exchanged in a day and 30 cycles will reduce the level of oxygen and $C0_2$ to a few parts per million at which point it will be possible to introduce the liquid argon stored in the buffer tanks into the detector tank. One outstanding question is the acceptable level of Nitrogen; this will be resolved in the small scale test setup.

The introduction of liquid argon into the detector tank produces a rapid reduction of the contaminants remaining in the tank atmosphere. Liquid at the surface is in equilibrium with the gas such that the relative concentration (by mass) of contaminants is the same in the liquid as in the gas. Because of the temperature gradients in the detector tank, the liquid in the tank will contain significant circulating currents which will continually bring new liquid to the surface to be exposed to the tank atmosphere. Given that the liquid density is $\sim$ 300 times the gas density, the majority of the contaminants are taken up by the liquid; the tank liquid purification system will then remove the contaminants.

The baseline for the tank purification system is two UltrAL [18] purifiers with a total capacity of 28 tons of liquid per hour, taking argon from the bottom of the tank and returning it near the top, operating continuously; we consider a tank filling rate of 150 tons per day. The evolution of the argon purity during the fill, once the contaminants in the tank atmosphere are removed, depends on several factors. These include the purity of the incoming argon, the outgassing from the walls and from the cable plant inside the detector, and the recirculation rate and effectiveness of the purification system. A program to model the evolution of the purity has been written [21] to give some insight into which are the critical parameters. Figure 5.5 shows the evolution of the purity in the tank, assuming on the left that the input argon purity is at 100 parts per trillion and on the right that it is 1000 parts per trillion.

It is clearly better to start with purer argon - the model tells us how much time we can gain (or lose). It can also be seen that the improvement effected by purifying

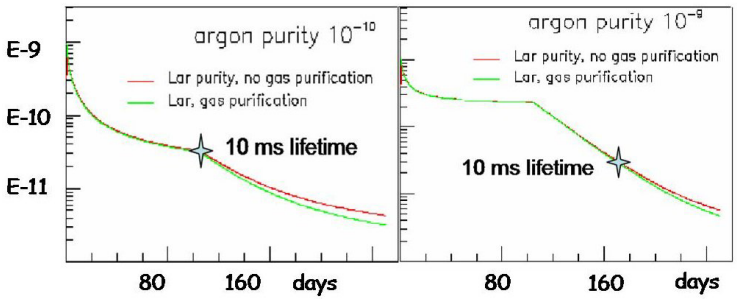

Figure 5.5: Evolution of purity of argon in the detector tank for different purities of incoming argon.

the gas volume directly is very small - a reflection of the fact that the liquid acts like a sponge on the contaminants in the gas.

5.3 Electronics and Data Acquisition

A minimum ionizing particle generates 55,000 ionization electrons per cm of path length in liquid argon. These electrons move in an electric field of 500 V/cm at a speed of ($v_{drift} = 1.5 mm/\mu s$) towards the readout wires where they produce signals on the two induction planes and on the collection plane. The signal will be reduced while drifting to the wires due to any O_2 or similar impurities. With 3 meters from cathode to signal wires, the maximum drift time is 2 ms and for an electron lifetime of 10 ms, the signal size is reduced by 20% for maximum drifts giving about 22,000 electrons per wire. The diffusion in liquid argon is given by $\sigma_{diffusion}(mm) = 1.0 \times (T_{drift}(ms)^{1/2})$ [4], typically 1 mm in our case.

We propose to use the ICARUS scheme [4] in which each signal wire is connected to a continuous wave-form digitizer operating at 2.5 MHz with 10 bits of dynamic range. The sampling rate is matched to the drift speed and diffusion, and the dynamic range allows a MIP in channel 20 with adequate range above for electron showers (typically only 4 particles) and for protons down to 100 MeV/c momentum. The major new issues for our situation are achieving adequate signal to noise given the long wires and cables used to bring the signals to the front-end electronics, and the architecture of the DAQ system. There is also the crucial issue of ensuring that the environment is not corrupted by auxillary equipment such as pumps, HV, and power sources, and that the signal paths avoid cross-talk and pick-up.

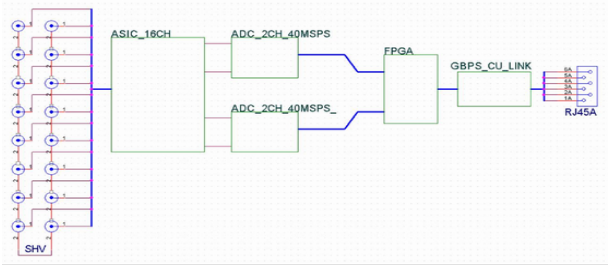

Figure 5.6: Schematic of electronics of 16 channels

5.3.1 Electronics

The active electronics attached to each wire include an amplifier-shaper (shaping time ~ 1 μs), an ADC to digitize the signal, an FPGA(Field Programmable Gate Array) to perform signal processing on the digitized wave-form, a small local memory and a serial link to transmit relevant data to the DAQ. Given existing commercial ADCs and the comparatively low digitizing rate, it turns out to be convenient to multiplex several input signals into a single digitizer. The ability to bias the wire at a few hundred volts and to inject test signals are also provided. The capacitance (to its neighbors) of each wire is ∼14 pf/meter; the capacitance of multi-conductor ribbon cable used to bring the signal from wire to front-end electronics is $\sim$ 50 pf/meter. For a 30 meter wire with 4 meters of interconnecting cable to the electronics, the total capacitance is 620 pF. As a demonstration that this situation is manageable, there exist commercial amplifiers (VA1CH,VAAsics [22]) with 1.25 μs shaping time and noise of $<$ 2500 electrons at this capacitance. This gives a signal to noise (S/N) of $\sim$ 9 which is adequate. In practice, we will investigate solutions where the very front-end amplifier, the dominant noise-source, is included in an ASIC and where it is made using discrete JFETs. It is planned to use commercial ADCs and FPGAs; their performance is adequate and their cost is low. We envisage a single electronics board will contain the processing for 128 channels. Figure 5.6 shows a schematic of 16 channels.

The purpose of the FPGA is to reduce the amount of data passed to the DAQ by distinguishing pedestals from data due to tracks. The ICARUS collaboration performed a careful study of signal shapes in order to achieve a successful implementation of such processing and we shall do the same. Figure 5.7 shows some raw signal samples from ICARUS. We envisage three modes of operation of the FPGA. In the simplest mode, the FPGA passes all the digitizings, the whole waveform train or WFT. In the next mode, it identifies consecutive digitizings rising above threshold, (DAT), and passes the next 40 samples. In the third mode, the FPGA does a

full signal reconstruction, (FSR), passing only a time and pulse area for each set of digitizings.

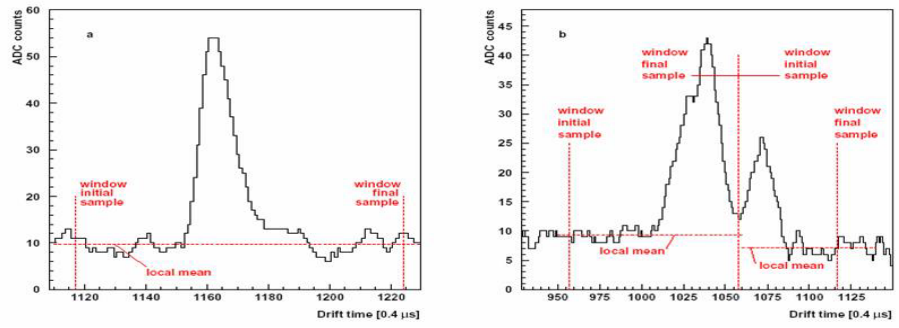

Figure 5.7: Raw digitizings from ICARUS TPC.

5.3.2 Data Acquisition

We first give some numbers corresponding to the three modes of signal processing described above. In WFT mode, the total data rate assuming 1 byte per digitization [23, 24] from the 110,000 active signal wires is $2.5 \times 10^6 \times 110,000 = 270$ GB/s. In the other modes, the vast majority of non-pedestal data should be due to cosmic rays which give a rate of 21.5 GB/s in DAT mode and about 2.5 GB/s in FSR mode.

There are two modes of operating the detector:

Spill Only In this mode the detector needs to be live only for the time needed to see events from the NuMI beam. Given a spill length of 10 μs and a drift time of 2 ms, we take this to mean the detector must be live for 3 ms each spill. We consider that the Main Injector will operate with a spill every 1.45 s after 2009.

Always Live In this mode the detector is always live.

A DAQ system based on commercial serial links, data concentrators, multiplexors and switches feeding a set of PCs has been designed by engineers in the Computing Division at Fermilab to achieve a DC rate of 5 GB/s. A schematic of the architecture is shown in Figure 5.8. This will allow the detector to run **Always Live** in FSR mode and **Spill Only** in WFT, DAT and FSR modes.

Table 5.2 summarizes the data rates for the different operating conditions.

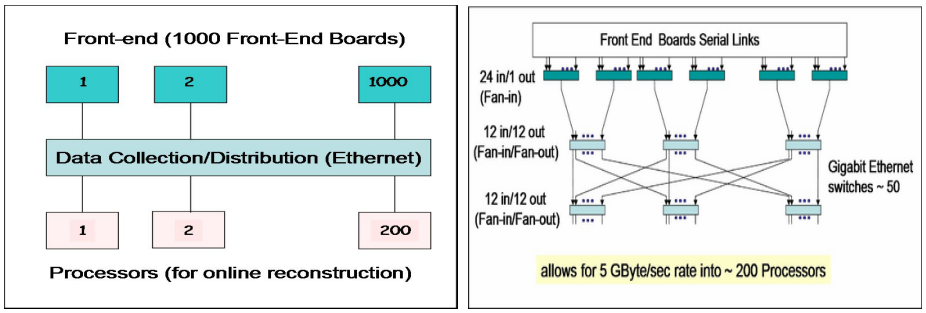

Figure 5.8: Schematics of DAQ system.

FPGA Mode	*Spill Only*	*Always Live*
WFT	*0.6 GB/s*	270 GB/s
DAT	*0.045 GB/s*	21.5 GB/s
FSR	*0.005 GB/s*	*2.5 GB/s*

Table 5.2: Data rates for **Spill Only** and **Always Live** operation with different in-line signal processing. Modes in italics are viable operating conditions

5.3.3 Cosmic Ray Data Rates

The cosmic muon rate on a tank of diameter 20 m and height 26 m is 100 kHz. Assuming a mean energy of 4 GeV, the cosmics will travel 20 meters in the tank - taking this as the average distance should be conservative. A 20 meter vertical muon will encounter at most 2000 angled wires of each orientation and some smaller number of vertical wires - so we take 5000 wires as the total number encountered. In the DAT mode, each track on each wire will result in 40 samples of 1 byte for each ADC value, 1 byte for wire address within a card, and 2 bytes for time giving $5000 \times 43 = 2.15 \times 10^5$ bytes per track and a total rate of $2.15 \times 10^5 \times 1 \times 10^5$ =21.5 GB per second. In FSR mode, the data generated per track per wire is 1 byte of wire address, 2 bytes of pulse area and 2 bytes of pulse time, giving a rate of 2.5 GB per second.

Chapter 6

Research and Development Towards the Baseline Concept

The use of liquid argon as a medium in an imaging detector is now a proven technique in particle physics. This idea has been developed from the original proposals and modest test setups of some 20 years ago [2, 25] to the large multi-ton setups of the ICARUS collaboration [4]. The baseline concept for a 15 kton detector described in Chapter 5 capitalizes on the successes of these developments.

However, a 15 kton detector raises new technical issues that must be addressed and understood before one embarks on such a massive construction project. The new issues can be broadly defined as being mostly the result of two factors:

- the scale of these massive LArTPCs
- the anticipated use of industrial techniques in building the cryogenic tank of this device.

These can be summarized in the following two questions:

- Can one build and operate the proposed detector's very long wire planes (20 m or longer)?
- Can one achieve the required argon purity (or equivalently the required electron lifetime) in a tank built utilizing materials and construction techniques commonly encountered in building industrial LNG storage tanks?

This chapter describes an R&D program to address these questions. While the focus of this program is towards a 15 kton baseline detector, the program addresses

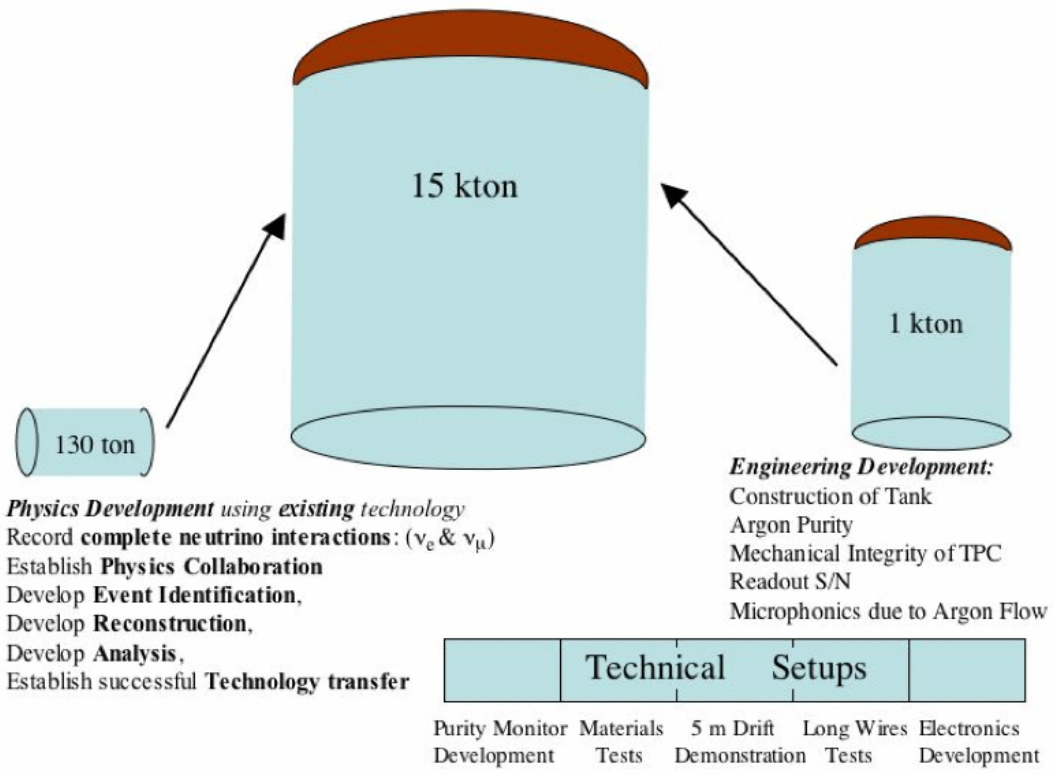

Figure 6.1: Proposed R&D program.

issues that will be faced by any multi-kiloton LArTPC detector. There are three main parts to this effort:

i. A number of technical test setups directed to answering specific questions pertaining to a massive LArTPC.

ii. The construction of a 50 ton fiducial mass (∼130 ton total argon mass) detector in which electron neutrino interactions can be fully reconstructed and a range of 2 GeV neutrino interactions studied. This detector will operate where it can obtain a sizeable number of neutrino interactions from the NuMI and/or Booster Neutrino beams.

iii. The construction and partial outfitting of a commercial tank of 1 kton capacity using the same techniques as proposed for the 15 kton tank. This will serve as the test-bed to understand the issues of industrial construction.

A schematic of the proposed R&D program is shown in Figure 6.1.

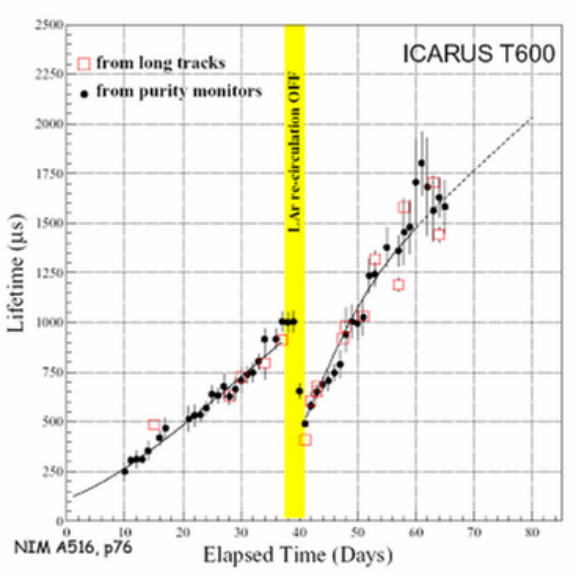

Figure 6.2: Comparison of electron lifetime in T600 as measured by the Purity Monitor and as measured by cosmic ray tracks, from [26].

6.1 Technical Test Setups

6.1.1 Purity Monitor Development

A device capable of measuring electron lifetimes in the range of 0.1 to ∼10 ms is necessary for carrying out many of the tests in this R&D plan. Furthermore many such devices will be used in any large detector setup as a process monitor of the purity of the liquid argon.

The purity monitor constructed by the ICARUS group [27] can serve this purpose. The purity monitor uses a flash of UV light to release a number of electrons from a photocathode; the electrons are then allowed to drift some distance under the influence of an electric field and the decrease in their number as well as their drift time are measured. The performance of this monitor has been verified [26] by ICARUS for lifetimes up to ∼2 ms as is shown in Figure 6.2. We will need to study this device and understand how we can extend its useful range.

This effort is already underway at Fermilab and is using an ICARUS purity monitor in its first tests.

6.1.2 Purification and Materials Test Setups

Filtering using the chromium based oxygen absorbing material Oxysorb™ was a major breakthrough in the ICARUS program that allowed the efficient purification of large volumes of argon in the liquid phase. Since that time, copper based materials and other proprietary oxygen absorbers have become available. Early studies have shown that these new materials outperform Oxysorb™. The evaluation of these new filtering media will be performed in a test setup which will also be used for the purity monitoring studies mentioned earlier.

The outgassing of oxygen and other electron absorbing impurities from the materials used in building large commercial LNG tanks (such as nickel steel) and of the materials to be used in building the wire chamber (such as signal cables, FR-4, G-10, Kapton, ball bearings, ...) will be the major long-term burden on the purification system. We are building a test setup to enable us to perform outgassing studies on these materials using a small test setup.

The ICARUS T600 detector, the largest LArTPC to date, and all its earlier prototypes were built in a clean room environment, utilizing clean room techniques, and were cleaned with processes used for UHV systems. In addition, before being filled with argon they were evacuated for some time to allow for the initial outgassing of their interiors. In our case the size of the detector precludes the option of the initial evacuation. Additionally, the large size and the long periods involved in the construction of the chambers will in all likelihood lead to a dirtier environment than the one encountered in the ICARUS detectors. We will therefore have to rely on the purification system to remove the initial and large impurity load. Studies of how well a purification system can respond to uncleaned surfaces, impurities (i.e. dirt), and outgassing are a major task of this initial R&D effort. The first setup of this effort is presently under construction at Fermilab.

6.1.3 Long Wire Test Setups

Long wire chambers present a variety of challenges. They are mechanical construction issues, issues of microphonic noise, and noise issues due to the intrinsic large capacitance of the wires.

To put this program in proper historical context, it should be noted that the largest LArTPC to date, the ICARUS T600, has a three plane readout with 3 mm spacing and 3 mm pitch. There is a first horizontal induction plane ∼9.4 m long,

followed by a second induction plane (at +30° from the vertical) ∼3.8 m long, and ending with a collection plane (at -30° from the vertical), also ∼3.8 m long. The baseline concept presented here has longer wires (∼25 m) but also larger plane separation and pitch (5 mm) leading to an amplifier input capacitance of ∼600 pF (vs. 230 pF and 110 pF for the two kinds of ICARUS T600 wire chambers).

The design choice described in this document for tensioning the wires is through the use of a weighting scheme that involves a doublet of pulleys. The usage of a weighting scheme is dictated by the fact that differential expansion and contraction during the various phases of the thermal history of the detector lead to large variations of the effective wire length (∼13 cm), which this scheme can accommodate more readily than a spring tensioning setup. Nevertheless, the large number of wires implies that any improvements on the stringing and tensioning methods will have significant impact on the cost of building the chamber. Because of this, other options are still being considered. We are in the process of building mock-ups to investigate these issues.

Dimensional stability of the wire planes, especially in the separation between the planes, is of some concern as portions of the induction planes are anchored on the tank walls. The dimensional stability of this scheme after cooldown remains to be evaluated. Alternative designs based on large picture frame style chamber supports will not have this problem but are costlier. These have not yet been fully considered.

Noise issues related to wire length are a primary concern. These arise from two sources. The first is noise induced by vibrations of the wires which characteristically shows up as a baseline shift with a frequency much lower than the one for true particle signals. The second is amplifier noise from the large input capacitances. In this case, the input capacitance is due to both the long wires and the long cable assemblies from the wires to the amplifier.

The study of these noise sources is a most important aspect of the initial R&D phase. The design of the front end amplifier is one significant part of this effort; the study of long wires in an environment simulating the one of the final detector is also being planned. We intend to have a setup with three wire planes consisting of a small number of wires forming a narrow and shallow but very long ($\geq$15 m) chamber. Initial noise studies with this chamber will be carried out in gas and warm liquid environments and the chamber will ultimately be operated with liquid argon as the active medium.

6.1.4 Long Drift and HV Test Setup

The longest electron drift distance in a LArTPC, at 1.4 meters, was in the ICARUS T600 setup [4]. Argon with sufficient purity to sustain an electron lifetime of 12 ms has been achieved [28]. The proposed ICARUS T1200 setup was desinged with drift distances of 3 meters and a test setup at CERN is under construction [29] with a drift distance of 5 meters.

This program must also establish the capability to drift electrons over such long distances. A long drift setup with modest transverse dimensions is envisaged to test electron drifts at distances comparable to the ones encountered in the baseline detector. This setup will also serve as a testing ground for HV feedthroughs and will also allow, in conjunction with the purity monitor studies, to develop techniques of measuring long electron lifetimes in liquid argon.

6.1.5 Small LArTPC chamber

A first small chamber with a fiducial mass of ∼0.1 tons that is a first attempt at building a small LArTPC capable of seeing tracks, doing purity tests, and understanding charge collection and light production is under construction at Yale University [30].

6.2 One Hundred Thirty Ton Prototype

Beyond the technical test setups described above, which are directed towards answering specific questions, we intend to also build two larger scale detectors that will help us answer questions more global in nature and will also address issues of detector integration, data acquisition, and data analysis.

One detector will have a fiducial mass of at least 50 tons of liquid argon (i.e. $\sim 36\text{m}^3$ or $(3.3\text{m})^3$) and a total mass of roughly 130 tons of liquid argon (i.e.: $\sim 93\text{m}^3$ or $(4.5\text{m})^3$).

This device will be constructed in a location on the surface at Fermilab in a position to see neutrinos from the NuMI and/or Booster Neutrino beamlines taking advantage of the large angle neutrino halo of these beams. In such a location a sizeable number of neutrino interactions can be observed, providing a unique sample of fully reconstructed electron neutrino interactions in LAr as well as other charged current and neutral current events. These events together with the cosmic ray events

that will also be collected will form a very valuable sample on which electronics, data acquisition, and analysis software can be developed. Such an enterprise will also allow a collaboration to coalesce, students to be trained, and it will allow us to develop and demonstrate our own hands-on understanding of this technology.

6.3 One Kiloton Prototype

A 15 kton detector is a factor 50 more massive than any single LAr device constructed to date. We are, moreover, proposing to construct this detector in a manner different from any previously assembled. The program of technical tests and development given above will let us develop techniques to be used for the purification of argon and for the construction and readout of very long wire chambers. We believe, however, that we should demonstrate that these techniques will work on a prototype tank of adequate size constructed using the techniques we propose for the final detector.

We consider a tank of one kiloton capacity as appropriate; such a tank has a characteristic length of 10 m compared to the final detector characteristic lengths of 25m (note that a 1(15) kton detector is a cylinder with a base diameter and height of 9.69(23.4) m). This one kiloton tank will allow us to show that we can achieve the required purity in a commercially constructed vessel and that our techniques for installing, positioning, and tensioning the wires allow them to survive the tank cooldown. Additionally, by successfully instrumenting and reading a number of wires - not necessarily a whole tank's worth - we will have a sizeable system demonstration before building the final detector. As illustrated in Figure 6.1, the issues to be addressed by the 1 kton and the 130 ton detectors are complementary. We plan to proceed with the 1 kton detector in parallel with the other efforts presented here.

6.4 Preliminary R&D Cost and Schedule

We have made an initial rough cost estimate for the R&D plan presented above. The technical test setups will cost approximately $595,000, the 130 ton prototype detector and its ancillary equipment approximately $1,530,000, and the 1,000 ton prototype approximately $3,630,000. These are M&S direct costs only. Table 6.1 shows a breakdown of these costs. These estimates will be refined in the near future as our engineering and design studies progress, and as we include costs in addition to M&S direct costs.

A preliminary schedule for this R&D effort is outlined in Table 6.2. The schedule shows completion of the prototyping program by January 2009, followed by tank construction until 2012. Data taking, as per schedule described in Chapter 2 begins mid-2012. We intend to invite and develop an international collaboration.

We recognize that this schedule is optimistic in that it is driven only by the technological considerations we are aware of at this time. There are no budget constraints imposed, and we assume that technical resources will be available as needed. Finally, the schedule as written here does not fold in the project management required for projects of this size.

Liquid Argon TPC R&D Cost Estimate

In thousands of US $ (FY05)

Technical Set-ups				
Purity monitor	80			includes scopes/labview
PAB purity and materials test setup	100			
Filters for other setups	50			e.g. for 5 m tests
Liquid argon inventory	10			excludes 5m test
Sub-total		240		
Long wire tests	40			includes 30m long cryostat
Wire and Cathode mock-ups (Lab E)	45			
Sub-total		85		
Five meter test				
Cryostat	70			
Cryogenic equipment	40			
Wire chamber, Field Cage	30			
Feedthrough (HV/Signal)	25			
Electronics	20			
Liquid argon inventory	10			
Sub-total		195		
Electronics development		75		
Total for test setups				**595**
130 ton neutrino detector (50 t fiducial)				
Liquid argon inventory	250			
Cryostat	750			
Wire chamber, Field Cage	150			
Electronics(4000 wires)	300			
Cryogenic equipment	40			
Feedthrough (HV/Signal)	40			
Sub-total		1530		
Total for 130 t (50t fiducial)				**1530**
1000 ton tank				
Tank (cryostat)	1500			
Liquid argon inventory	1500			
Cryogenic equipment	100			
Argon purification	250			
Wire chamber, Field Cage	200			
Feedthrough (HV/Signal)	40			
Electronics(500 wires)	40			
Sub-total		3630		
Total for 1000 ton tank				**3630**
R&D Grand Total				**5755**

Table 6.1: Breakdown of preliminary costing for R&D program. Only M&S costs related to the detector hardware R&D at Fermilab are shown. Operations costs are not shown.

130 ton Prototype	Long wire test setup and 1 kton prototype	15 kton detector	Date
Start R&D on front-end electronics, HV feedthroughs, purity monitors, 3m drfit	Start R&D on long wires	Develop tank and electrode design	Jan 2006
			June 2006
TDR for 130 ton prototype	TDR for 1 kton tank		Jan 2007
End of R&D on front-end electronics, HV feedthroughs, purity monitors, 3m drift. Start of 130 ton prototype construction	Start construction of 1 kton tank	Finish conceptual design, start process of DOE project approval	June 2007
			Jan 2008
End of 130 ton prototype construction. Start of data taking using surface ν beam	End of 1 kton tank construction. Start filling with LAr	TDR	June 2008
Observation of ν interactions in 130 ton prototype	End of tests on 1 kton tank		Jan 2009
		Get final approval and start civil site preparation	June 2009
		Start of tank construction	Jan 2010
			June 2010
		End of tank construction, start of detector construction	Jan 2011
			June 2011
		End of detector construction, start of LAr filling	Jan 2012
		Start of data taking	June 2012

Table 6.2: Preliminary schedule for R&D program leading up to data taking in 2012.

Chapter 7

Cost Estimate for a 15 kton Detector

The cost of the detectors for electron neutrino appearance experiments is an important, perhaps even deciding, issue for the whole off-axis program, and the relative costs of the argon ionization and the scintillator light based technologies need to be properly understood. The state of the liquid argon cost estimate is preliminary but we can see the main cost-drivers and for some of these we already have a good estimate. The costs given throughout do not include EDIA or contingency.

7.1 Detector Considerations

It may be useful to identify some of the features that distinguish the liquid argon TPC (LArTPC) approach and the scintillator design. There is, for example, a large difference in the number of channels for a given detector 'mass × efficiency' between scintillator and liquid argon. For a NOνA style liquid scintillator, it takes 2 tubes (one horizontal, one vertical) to define an x,y,z point and so 1 channel corresponds to a volume of 1 tube which is ∼40,000 cm^3($5 \times 5 \times 1600$) cm^3. In the 15 kton LArTPC detector, an x,y,z point is defined by two channels which cover a volume of 300,000 cm^3($0.5 \times 300 \times 2,000$) cm^3 (wire spacing × drift distance × height of wires). (In fact, there are regions where the readout is overconstrained (3 channels) so we have about 2.5 channels per 300,000 cm^3 or 120,000 cm^3 per channel.) The net result is that the volume per channel in argon is effectively 3 times the volume per channel in

scintillator (120,000 cf 40,000 cm^3).

Two more effects affect the channel ratio. One effect is the higher density of liquid argon, a factor of 1.4, which turns the 3 above into 4; the second is the higher efficiency for event recognition in the liquid argon. NOνA [31] gives its efficiency as $\sim$ 30%; liquid argon claims an efficiency of about 80%. If we take a factor of 2 relative efficiency, the overall factor for a liquid argon 'channel' compared to a scintillator 'channel' is about 8 (4×2). This bottom-up calculation is consistent with a simple top-down calculation. If one assumes the sensitivity ratio of 2, a 15 kton LArTPC detector is equivalent to a 30 kton scintillator device and one can compare the numbers of channels, which are 100,000 for LAr and 760,000 for NOνA.

This difference affects many aspects of the cost. One needs to procure 8 times the number of fibers and plastic tubes as wires, and one needs to assemble 8 times as many tubes with their fibers, photodetectors and readout electronics for a scintillator design as for the LArTPC. The NOνA detector and building base cost is $\sim$ \$86 million [32]. Our estimate for the comparable LArTPC detector and building cost is $\sim$ \$57 million (2005 \$) of which \$26 million are the liquid argon tank and the argon itself, costs which are expected to be reliably estimated since they are based on standard industrial products.

7.2 Mechanical Infrastructure Costs

Table 7.1 gives the costs associated with the construction of the tank equipped with the TPC. The costs are estimates from the Fermilab PPD mechanical engineers, except where stated in the comments.

Item (15 kton)	cost (k$)	Comment
Site Preparation	5,300	same as NOvA
Buildings	2,000	support buildings only
Tank	13,300	e-mail quote
Habitable Deck	2,500	$300/sq ft.
Tank Top Structure	4,000	Wire Load/Tank Pressure
Cathode and Field Cage	3,000	Eng. Estimate
Signal Planes	3,000	Eng. Estimate
Access to Deck	1,500	Elevator and Stairways
Assembly Platforms	1,000	Installation of TPC
Total	**35,600**	

Table 7.1: Estimate for Mechanical Infrastructure

7.3 Cryogenic Systems

Table 7.2 gives the cost of the cryogenic systems, including the argon receiving stations, the argon purification system and the nitrogen system for cooling the argon. The cost of the cryogenic systems is dominated by the argon itself, which is included here.

Item (15 kton)	cost (k$)	comment
Argon	13,000	2004 quote
LAr purifiers	800	Commercial (includes spare)
Tank atmos. purification	500	eng. estimate
LAr Receiving & Transfer	1,500	3 stations
LAr Instrumentation & Controls	250	Commercial Software/Hardware
LN_2 Storage and Pumps	300	includes back-up
LN_2 Instrumentation & Controls	100	Commercial Software/Hardware
Heat Exchangers	100	eng. estimate
Total	**16,550**	

Table 7.2: Estimate for Cryogenics Material and Systems

7.4 Detector Electronics

The continuous waveform electronics and the data-acquisition system for the LArTPC detector are well matched to modern commercial technology. The very front-end amplifier and the front-end shaper are indeed special devices which will require careful and specific design. For the rest of the electronics readout, however, commercial devices are just fine. Commercial ADCs can be used to digitize the signal, commercial FPGAs can be used to process the numbers and the Data Acquisition System is based on commercial switch systems from the communications industry. We have costed existing commercial devices shown in Table 7.3; it will be noticed that the passive components (connectors, cable and printed-circuit boards) are estimated to cost as much as the active components.

Item (15 kton)	cost (k$)	Comment
Front-End ASIC	1,000	ASIC development & production
Commercial Components	500	ADC, FPGA and Data Link
Connectors, cable, PC Boards	1,100	Parts & similar boards
Feedthroughs	300	Purchasable Devices
Power Supplies	200	
Total	**3,100**	

Table 7.3: Estimate for Electronics

7.5 Data Acquisition and Control

Table 7.4 shows costs for the DAQ and controls systems. These numbers come from a system design made by Fermilab Computing Division engineers. The design was developed from the proposed BTeV DAQ system and is based on standard components from the telecommunication industry.

Item (15 kton)	cost (k$)	Comment
Switches & cable	50	Commercial Product
Computers	500	200 PCs
Slow Controls	200	Eng. Estimate
Timing System	100	Eng. Estimate
Data Storage	1200	2 Pbytes[1]
Development Systems	200	Eng. Estimate
Total	**2,250**	

Table 7.4: Estimate for Data Acquisition

7.6 Total Costs

The costs presented in this chapter add up to a total of 57.45 Million dollars. This is a preliminary cost estimate which does not include EDIA or contingency.

[1]Enough for 1 year of DAT data (Data Above Threshold ,see Data Acquisition Section)

Chapter 8

Additional Physics Opportunities with Large Liquid Argon Detectors

A 15 kton liquid argon detector, the baseline concept of this document, would provide a timely capability to study the neutrino mass hierarchy and $\sin^2 2\theta_{13}$ in a long-baseline neutrino beam. This capability is by itself sufficient justification for construction of such a detector, but it by no means exhausts the promise of this technology. Here we briefly review some of the many ways in which large liquid argon detectors could address additional physics topics in both accelerator and non-accelerator "beams".

8.1 Accelerator-Based Physics Opportunities

8.1.1 Physics with a Liquid Argon Near Detector

A long-baseline neutrino physics program with a large liquid argon detector should, of course, include a liquid argon near detector to aid in the characterization of the neutrino beam, and to increase our understanding of neutrino-argon cross sections at the relevant energies.

The near detector should have the capability of reconstructing the energies of both electron-neutrino and muon-neutrino events, and so should operate in conjunction with an external muon identifier, such as in the MINERνA project at Fermilab [33] and the 2-km near detector option at J-PARC [7].

8.1.2 Physics with a Second Liquid Argon Far Detector

Measurements of neutrino-oscillation parameters in long-baseline neutrino experiments are subject to well-known degeneracies whose resolution will require the use of multiple neutrino energies and/or detectors at multiple baselines. It is too early to discern the optimum strategy for this effort, but it is surely needed.

If off-axis neutrino beams are to be used, then only one neutrino energy is favored at a given baseline, so there is a need for detectors at more than one baseline. A recent example of the physics case for this option has been given by Mena *et al.* [34]. In a program based on an existing neutrino beam such as NuMI, it is favorable to place one detector at a longer than nominal baseline and the other at a shorter baseline, and at appropriate transverse distances to the nominal beamline so that both detectors observe a peak in the resulting "off-axis" neutrino spectra.

If, however, it is favored to use only a single detector site, then the neutrino beam should not be an off-axis beam, but rather on-axis and broad band so that multiple oscillation peaks can be studied [35]. It has been suggested that the high energy tail of a wide band beam would be an ideal place to look for Lorentz Invariance Violation in $\nu_\mu \rightarrow \nu_e$ appearance [36]. Of course, it remains favored to use the largest possible neutrino detector, so the evolving physics interest may lead to the construction of a second, large liquid argon detector at the same site as that of the initial detector.

A variant that combines the advantages of narrow-band neutrino beams and a single detector site is to use neutrinos from a solenoid horn, rather than from a toroidal horn [37], since a solenoid lens is capable of point-to-parallel focus at multiple momenta. However, neutrinos from a solenoid lens are not sign selected, so the neutrino detector must include a magnetic field to determine the sign of the final-state leptons. A liquid argon detector is perhaps the only option for a large, magnetized neutrino detector that could observe the sign of both electrons and muons, although realization of this option is beyond the scope of the present document.

8.1.3 A Magnetized Liquid Argon Detector at a Neutrino Factory

If the neutrino oscillation parameter $\sin^2 2\theta_{13}$ is much smaller than 0.01, it will be extremely difficult to measure this, and the CP-violation parameter δ, with muon-

neutrino beams from pion decay, due to electron-neutrino backgrounds from decays of muons. If instead the neutrinos come from the decay of positive muons of a well-defined energy in a storage ring [38], then muon neutrinos and electron anti-neutrinos (or muon anti-neutrinos and electron neutrino from negative muons) are obtained with well-known energy spectra and essentially no "wrong-sign" backgrounds. However, the sign of the final-state muons in the neutrino interactions must be determined by the detector to distinguish the two types of neutrinos in the beam.

A magnetized liquid argon detector in a long-baseline neutrino beam from a so-called "neutrino factory" could measure 12 types of neutrino oscillations, and observe both CP- and T-violating asymmetries for values of $\sin^2 2\theta_{13}$ as low as 0.0001.

8.2 Non-Accelerator Physics Opportunities

One of the earliest visions of a (magnetized) very large liquid argon detector emphasized its utility for measurements of proton decay, atmospheric- solar- and supernova-neutrino astrophysics, as well as for long-baseline accelerator neutrino physics [39]. It is, however, problematic whether any of these physics topics could be addressed unless the detector were sited underground.

Of the non-accelerator physics topics accessible to a large liquid argon detector, the most fundamental is the question of proton decay, which was a motivation for Rubbia's initial consideration of this technology [2]. Of particular interest is the capability of a liquid argon detector to reconstruct such decays as $p \rightarrow \bar{\nu} K^+$, for which the efficiency of a water Čerenkov detector is very small, but which modes are favored over $p \rightarrow e^+ \pi^0$ in a significant class of theories of proton decay.

A very large, magnetized liquid argon detector would also be capable of using atmospheric neutrinos that have crossed through the Earth to resolve the mass hierarchy problem for moderately large values of $\sin^2 2\theta_{13}$ [40].

Chapter 9

Summary and Conclusions

Remarkable and startling discoveries in the past decade are generating a growing excitement in neutrino physics. Understanding the masses and mixings and searching for CP violation in the neutrino sector are pressing questions. The 2005 APS Neutrino Study has identified, in their highest recommendations, long-baseline, off-axis physics as the way to explore these parameters [1].

The newly commissioned NuMI beamline at Fermilab provides the most intense neutrino beam available for this physics. Still, ν_e appearance searches suffer from low statistics and large background contamination necessitating large detectors and long run-times. The LArTPC detection technique, with excellent ν_e efficiency and neutral current π^0 rejection maximizes sensitivity to this physics coupling the best detector with this intense beam.

The path to realizing massive LArTPCs for this program involves an R&D program, laid out in this document, on an achieveable but aggressive timeline. This R&D program includes parallel study of neutrino interactions in a small ($\sim$ 130 ton) LArTPC as well as engineering studies of industrial scale techniques in a 1 kton vessel. The program addresses the most pressing R&D questions including understanding purity, the mechanics of long wires as well as providing a test bed for design of electronics, DAQ, TPC, etc. Finally, a small data set of neutrino interactions at $\sim$2 GeV allows for study of different interactions as well as unfolding of beam events from cosmic ray interactions.

The success of this R&D program keeps this effort on a path to begin data taking in 2012, as per Pier Oddone's timeline shown in Chapter 2. The success of this

program will bring together the world-class NuMI beamline with the best possible detectors, and a great opportunity to continue exploration in the neutrino sector.

Bibliography

[1] "A Joint Study on the Future of Neutrino Physics: The Neutrino Matrix", APS Multidisciplinary Neutrino Study (November, 2004), http://www.aps.org/neutrino/index.cfm

[2] C. Rubbia, "The Liquid-Argon Time Projection Chamber: A New Concept For Neutrino Detector", CERN-EP/77-08 (1977).

[3] A. Para, "Reply to the Initial Set of Comments and Questions", Fermilab PPD Mini-Review (April 19, 2005), http://www-off-axis.fnal.gov/notes/public/ppt/flare0050/flare0050.ppt

[4] S. Amerio *et al.* [ICARUS Collaboration], "Design, construction and tests of the ICARUS T600 detector," Nucl. Instrum. Meth. A **527**, 329 (2004).

[5] A. Para, "Challenges of a Large Liquid Argon Detector", Fermilab PPD Mini-Review (April 5, 2005), http://www-off-axis.fnal.gov/notes/public/ppt/flare0046/flare0046.ppt

[6] P. Rapidis, "R&D Plan and Request for Resources", Fermilab PPD Mini-Review (April 19, 2005), http://www-off-axis.fnal.gov/notes/public/ppt/flare0046/flare0046.ppt

[7] E. Kearns *et al.*, "A Proposal for a Detector 2 km Away From the T2K Neutrino Source", (May 20, 2005), http://www.phy.duke.edu/~cwalter/nusag-members/

[8] P. Oddone, "A vision for Fermilab", presentation to the National Academy Panel, EPP2010 (May 16, 2005), slide 34, http://www7.nationalacademies.org/bpa/EPP2010_Presentation_Oddone.pdf

[9] F. Arneodo *et al.* [ICARUS Collaboration], "The ICARUS 50-l LAr TPC in the CERN nu beam," arXiv:hep-ex/9812006.

[10] P. Cennini *et al.*, "Performance of a 3-ton liquid argon time projection chamber," Nucl. Instrum. Meth. A **345**, 230 (1994).

[11] F. Arneodo *et al.*, "Performance of the 10-m**3 ICARUS liquid argon prototype," Nucl. Instrum. Meth. A **498**, 292 (2003).

[12] O. Mena and S. Parke, "Physics potential of the Fermilab NuMI beamline," arXiv:hep-ph/0505202.

[13] Robert Hatcher and Adam Para, http://www-off-axis.fnal.gov/flare/index.html.

[14] H. Gallagher, *AIP Conf. Proc*, **698**, 153–157 (2004).

[15] Adam Para, presentation to the 2nd FNAL Review on LAr detectors. April 2005.

[16] R. L. Schmitt, FLARE note 60, 2005

[17] E. Buckley *et al.*, "A Study Of Ionization Electrons Drifting Over Large Distances In Liquid Argon," Nucl. Instrum. Meth. A **275**, 364 (1989). F. Arneodo *et al.*[ICARUS collaboration],"The ICARUS Experiment", LNGS-EXP 13/89 add.2/01 (November 2001)

[18] Air Liquide UltrAL^{TM}, capacity 14 tons/hour

[19] G. Carugno, B. Dainese, F. Pietropaolo and F. Ptohos, "Electron Lifetime Detector For Liquid Argon," Nucl. Instrum. Meth. A **292**, 580 (1990).

[20] S. Amoruso *et al.*, "Analysis of the liquid argon purity in the ICARUS T600 TPC," Nucl. Instrum. Meth. A **516**, 68 (2004).

[21] This and many aspects of the description come from A. Para, FLARE note 56, 2005

[22] see http://www.ideas.no/products/ASICs/pdf/VAAsics.pdf

[23] This scheme uses 1 byte per reading even though the ADC returns 10 bits by reporting the differences between successive values. Reserving a sign bit and a bit for cases where the difference is too great allows for 6 bits of difference. Cases where the difference is greater than 63 must be handled correctly but are very rare and hardly affect the total amount of data transferred.

[24] S. Amerio *et al.*, "Considerations on the ICARUS Read-out and on Data Compression", ICARUS-TM/2002-05.

[25] H. Chen *et al.*, *Nucl. Inst. Meth.* **150**,(1978) 585.

[26] S. Amoruso *et al.*, *Nucl. Inst. Meth.* **A516**,(2004) 68 .

[27] G. Carugno *et al.*, *Nucl. Inst. Meth.* **A292**,(1990) 580; A. Bettini *et al.*, *Nucl. Inst. Meth.* **A305**,(1991) 177; see also [4] .

[28] A. Bettini *et al.*, *Nucl. Inst. Meth.* **A315**,(1992) 223; F. Arneodo *et al.*, presentation at the INFN Eloisatron Project: 36th Workshop: New Detectors, Erice, Italy, 1-7 Nov 1997, hep-ex/9812006; see also ICARUS collaboration P. Aprili *et al.* Unpublished Report ICARUS-TM/2001-09 and CERN/SPSC 2002-027 (2001) page 21.

[29] F. Sergiampietri and D. Cline, private communication; A. Bueno *et al.* LANDD-5MD. R&D Proposal CERN-SPSC-2004-033, CERN-SPSC-I-230, Sep 2004.

[30] See http://hepwww.physics.yale.edu/nup/

[31] NOvA Proposal March 21 2005, hep-ex/0503053, NOvA Collaboration, D. Ayres *et al.*

[32] *ibid.* p 105, items 1.0 and 3.0 without shipping charges (1.3) and site work (3.1).

[33] D. Drakoulakos *et al.*, "Proposal to Perform a High-Statistics Neutrino Scattering Experiment Using a Fine-grained Detector in the NuMI Beam", (Dec. 23, 2004).

[34] O. Mena Requejo *et al.*, "Super-NOvA: a long-baseline neutrino experiment with two off-axis detectors", (Apr. 3, 2005), hep-ph/0504015

[35] M.V. Diwan *et al.* "Very Long Baseline Neutrino Oscillation Experiments for Precise Measurements of Mixing Parameters and CP Violating Effects", Phys. Rev. D **68**, 012002 (2003).

[36] F. R. Klinkhamer, Phys. Rev. D **71**, 113008 (2005) [arXiv:hep-ph/0504274].

[37] K.T. McDonald, "A Neutrino Horn Based on a Solenoid Lens" (Dec. 1, 2003), physics/0312022

[38] M.M. Alsharo'a *et al.*, "Status of Neutrino Factory and Muon Collider Research and Development and Future Plans", Phys. Rev. ST Accel. Beams **6**, 081001 (2003).

[39] D.B. Cline *et al.*, "LANNDD – a massive liquid argon detector for proton decay, supernova and solar neutrino studies and a neutrino factory", Nucl. Instr. and Meth. **A503**, 136 (2003).

[40] R. Gandhi *et al.*, "Earth Matter Effects at Very Long Baselines and the Neutrino Mass Hierarchy", (Nov. 19, 2004), hep-ph/0411252